



Journal of Mining and Environment (JME)

journal homepage: www.jme.shahroodut.ac.ir



Cavability Assessment of Rock Mass in Block Caving Mining Method based on Numerical Simulation and Response Surface Methodology

Behnam Alipenhani, Abbas Majdi*, and Hassan Bakhshandeh Amnieh

School of Mining Engineering, College of Engineering, University of Tehran, Tehran, Iran

Article Info

Received 25 April 2022

Received in Revised form 23 June 2022

Accepted 30 June 2022

Published online 30 June 2022

[DOI:10.22044/jme.2022.11858.2176](https://doi.org/10.22044/jme.2022.11858.2176)

Keywords

Block caving

Numerical modeling

Joint characteristics

UDEC software

Response surface methodology

Abstract

The present work aims at implementing Response Surface Methodology (RSM) in order to generate a statistical model for Minimum Required Caving Span (MRCS) and estimate both the individual and mutual effects of the rock mass parameters on rock mass cavability. The adequate required data is obtained from the result of numerical modeling. In this work, various arrays of numerical simulations (480 models) are carried out using the UDEC software in order to study the rock mass cavability thoroughly. The effect of each individual parameter and their mutual effect on MRCS are investigated by means of ANOVA. ANOVA indicates that all the chosen parameters (depth, dip of the joint, number of joints, angle of friction of the joint surface, and joint spacing) highly affect MRCS. In other words, the results of ANOVA are in high agreement with the results of the conventional sensitivity analysis. Moreover, a combination of joint spacing and joint inclination has the highest mutual effect on MRCS, and a combination of undercut depth and joint spacing has the lowest effect on MRCS.

1. Introduction

Block caving mining is the most preferred underground mining method due to low operation cost and high productivity. Such a method provides a higher safety compared to the other operations and offers greater flexibility than any new technology such as autonomous operation. Cavability is one of the most significant factors in implementation of block caving mining [1]. Cavability of rock mass refers to the initiation, propagation, and continuity of caving [2]. The onset of the caving process and its propagation during the mining activity is a key influential factor that has a direct impact on mine productivity [3].

Since the application of caving methods dates back to before the twentieth century, much research has been done in order to understand and predict the nature of caving propagation. Rice [4] and later Panek [5] have developed a simple one-dimensional (1D) volumetric method to investigate

the properties of caving propagation behavior assuming volume increase coefficients. Today, simple volume relationships are still used by many researchers to estimate the rate of caving propagation (e.g. Beck [6]). The hypotheses considered in this method are: 1) Caving initiations always happen; 2) The propagation of caving (and movement of material) is always vertical; 3) The caving rate is constant (based on the use of a constant volume increase coefficient). Several case studies later showed that these assumptions were incorrect. Studies by Beck [6] at the Ridgeway Deeps Mine in Australia have shown that sometimes caving initiations may not occur on part of the undercut area. Carlson and Golden (2008) [7] at the Henderson mine observed a situation where the propagation of caving occurred farther from the undercut area and along a loose surface. At the Northparkes mine, Ross and van (2005) [8]

✉ Corresponding author: amajdi@ut.ac.ir (A. Majdi).

observed highly variable caving rates at the time of onset, propagation, and cessation of caving.

Somehneshin [9] had some assumptions and used these assumptions for estimation of the optimized length and width of block. The explored relationship was analyzed using MATLAB, and the resulting graphs thereof were drawn. In the Somehneshin research work, the previous assumptions were also considered, which, as mentioned, may not be true. Rafiee [10, 11] used a rock engineering system (RES), which analyzes the interrelationships between the effective parameters to study the cavability of rock. He also used a fuzzy system to minimize the subjectivity of weights calculated in the RES method. The main limitation of the analytical approaches is that they take few details of rock mass geo-mechanical conditions into consideration.

In 1980, Mathews [12] proposed an empirical method for evaluating the stability of open stopes, one of the applications of which was to determine the cavability of the deposit. In this method, like the Laubscher method, the cavability was related to the hydraulic radius. A stability graph is obtained from the relationship between hydraulic radius (S) and stability number. The N Mathews stability graph has been modified and updated several times with the addition of more data. One of these modifications was made by Potvin [13], which resulted in the modification of the stability number and the transformation of the first three regions into two stable and caving regions. In 1990, Laubscher [14] developed the most commonly used method for estimating cavability based on a combination of data from large mines in South Africa. Using this chart and determining the mining rock mass rating (MRMR) and the hydraulic radius of the deposit footprint, the status of the rock mass can be determined.

Other limitations: The empirical method of Laubscher and Madsley have already been documented by Brown [1], and he believes that the empirical method is only satisfactory for the length-to-width ratios of three or less. On the other hand, this technique is not able to calculate the 3D stress redistribution changes around a rectangular section. In addition to the effects of orientation, only one seam can be analyzed. Experience has shown that the orientation of the critical joint can change around the shear when the direction of the main stress changes during undercutting and propagation of caving. Milne [15] also stated that the determination of adjustment coefficients can be ambiguous and dependent on the personal experience. This means that for a similar dataset

from a rock mass, different caving behavior may be interpreted. In addition, the use of empirical methods does not provide us with information about the rate of propagation of caving as well as the extent of the behavioral zones of caving. As a result, the empirical method has been obtained from a limited series of data to the past, and therefore, their application in reserves with large-scale caving, anisotropic rock mass strength, and heterogeneous masses is limited.

Nowadays due to the advancement of high-speed computers, numerical simulation has become more popular for the assessment of complex geo-mechanical problems such as rock mass cavability.

The first 2D elastic finite element model was introduced by Palama and Agarwal [16] to study the caving progress at the El Teniente mine in Chile. Then they could identify the application of computer numerical modeling in the analysis of caving propagation and provide a tool for further mathematical analysis of the mechanism of tensile failure forming by the progress of caving. However, their study was based on a simple model of elastic material, which was not able to explain the mechanism of stress caving owing to not defining the failure criterion. Lorig [17] has performed simulations in axisymmetric models to better indicate the 3D shape of the caving propagation and the surrounding induced stresses. In these models, the sub-section of a cylinder located at great depths was investigated. The initial state of stress within the model was assumed to be caused by the weight of the floors, and it was introduced on the undercutting floor to provide the initial stability of the boundary stresses (a support pressure). Flores and Karzulovic (2003) [18, 19] in an international study on caving (1997-2004) assessed the effect of depth, stress, large-scale discontinuities, the strength of rock mass, and groundwater on cavability by the finite element method (conceptual models). They also used the assumption of vertical caving propagation similar to an analytical method. In order to estimate the propagation potential of the caving, it was assumed that the caving propagation would be equal to 10% of the length of undercutting (for example, for the undercutting length of 100 m, the vertical caving propagation would be 10 m). They proposed a propagation coefficient (CPF) for caving to determine whether the caving is probable, transient, or spontaneous, which is very similar to the transition and stable areas of Laubscher. CPF was defined as the ratio between the difference of the main stresses in the caving area and the

maximum difference of the stresses that the rock mass can withstand.

Pierce [20] could simulate the caving behavior involved in the Northparkes mine three-dimensionally as FEM/DEM-DFN have been adopted by many researchers. The Synthetic Rock Mass (SRM) approach that was introduced by Candal has opened a new area in the modeling of rock mass. This method brings two well-established techniques together: a) The Bonded Particle Model (BPM) [21] for the simulation of intact rock deformation and brittle fracture b) the Discrete Fracture Network (DFN) in which joints are represented by Smooth Joint (SJ) model for the representation of the rock mass *in situ* joint fabric [20]. Sainsbury [22] has studied the effect of stress direction relative to undercutting on cavability. Kyu-Seok Wooa [23] have used FLAC3D to assess the settlement in the Palabora mine.

Raffie [24] has investigated the effect of seven parameters, the compressive strength of intact rock (UCS), joint orientation, joint persistence, joint density (P32), joint friction, confined stress, and hydraulic radius (HR) using numerical. In order to assess the influence of each parameter in numerical modeling, the value of one parameter is changing while the values of other six parameters are fixed. The in-situ stress and hydraulic radius are the most effective parameters involved in cavability of rock mass in block caving mines.

Xia [25] has established a numerical simulation model in FLAC3D software using weak undercutting operations considering the actual observations and physical parameters of the mine. They found that under the high in situ horizontal shear stress and with the progress of undercutting, a huge deal of stress is gradually created in the extraction layer. In this way, the compressive stress and tensile stress are concentrated on the upper and lower parts, respectively. By the progress of the undercutting in the remaining ore column, stress release occurs in the upper part of the undercutting floor, which hardens the ore's motion and reduces the recovery.

Xia *et al.* [26] has developed a numerical simulation model using the FLAC3D software with the Mohr-Coulomb strength criterion. They analyzed and controlled the stress situation on the components of the extraction layer separately after each step in the large caving method. They indicated that undercutting in the main sub-floor could reduce the probability of secondary ground pressure damage. The results of this study can be useful for directing the mineral to the extraction

layer slowly and without serious damage in the large caving method [20].

In 2020, numerical modeling was performed by Wang *et al.* [27] at the Beijing University in China in order to investigate the effect of the standard block size on the caving mechanism using the PFC software with 9 different sizes. The standard block size is divided into two stages: the uniform distribution stage (UDS) (uniform distribution stage) whose value is less than 0.1, and the non-uniform distribution stage (NDS) whose value is more than 0.1. This experiment examined changes in the recovery ratio, final shape drawing, top coal boundary, and contact force between the particles. The experimental results showed that the recovery ratio increased with increasing standard block size first and then decreased in UDS. This study provided a basis for predicting the recovery ratio, and showed that coal was more uniformly controllable and had a higher recovery ratio.

Mohamadi *et al.* [28] have presented a hybrid probabilistically qualitative–quantitative model to evaluate cavability of immediate roof and to estimate the main caving span in longwall mining by combining the empirical model and the numerical solution. For this purpose, numerical simulation was incorporated to Roof Strata Cavability index (RSCi) as summation of ratings for nine significant parameters. A distinct element code was used to simulate numerically the main caving span corresponding to various RSCi classes probabilistically.

Physical modeling was first used by Lehman in 1916. McNicholas *et al.* [29] in 1946 studied recovery at the Miami Copper and Climax molybdenum mines in the United States. They studied the effects of draw point spacing on the recovery. McNicholas concluded that in the case of coarse caved material, the distance from the draw point should be wider than in the case of fine material.

In 2012, physical modeling was performed by Carmichael and Hebblewhite [30] at the University of New South Wales to analyze crack propagation and areas formed in the large caving extraction method. The materials used in this modeling were sand, sand, and plaster. The dimensions of this model were 1 m length, 1.25 m height, and 0.188 m thickness. The results of this modeling showed that synthetic rock mass could be used in large block caving modeling.

In 2016, Potvin and Wesseloo [31] accelerated the physical model of gravity to the g80 using a geo-technical centrifuge. By accelerating to several times the gravity of the earth, the experiment

represents a state several times the actual size of the sample, as described in the Hoek's law of scale (1965). The experiments were two-dimensional, and an on-screen DSLR camera made it possible to visually observe the demolition behavior. The results of these experiments showed that the caving propagation could occur through a series of fractures parallel to the caved back and progress as a "jump" to parallel and vertical failure. In this article, this mechanism was called fracture banding.

In general, several rock mechanical indices are used in the assessment of cavability such as RQD, MRMR, and N. Many of these indices are obtained from mines, and thus they are mine-dependent. Secondary blasting is one of the empirical indices in which the number of explosions has an inverse relationship with the accessible fragmentation degree during the caving process. As a rule of thumb, when 50% of the particles of the broken rock mass are in the range of less than 1.5 m, then it could be helpful to determine the cavability of the rock mass as an important criterion [13]. Applying Rock Quality Designation (RQD) is another approach for the evaluation of rock mass cavability [32]. In 1990, a new state-of-the-art approach was introduced by Laubscher [14], which was developed based on the caving data gathered from the underground mines in South Africa. In that approach, a chart was proposed to predict cavability of rock mass based on Mining Rock Mass Rating (MRMR) and hydraulic radius of the undercut [33]. Later in 2000, Laubscher and Jakubec [34] modified the original chart leading to the elimination of RQD from cavability assessment. They argued that RQD was unable to have an accurate estimation of rock mass quality [14]. Although such a method was found to be suitable for cavability assessment of weak and large rock masses, its accuracy is largely dependent on rock mass homogeneity as well as the quality of the input data used for estimating MRMR. Furthermore, the modified chart proposed by Laubscher and Jakubec [34] for higher values of MRMR (e.g. MRMRs greater than 55) and small volumes of rock mass resulted in a significant discrepancy between the predicted cavability assessment and that observed in the field [22].

The Mathews stability diagram was developed based on the relationship between the hydraulic radius of undercut and the stability number (N) [35]. The proposed diagram has a number of limitations; it was not a factor in the block caving method. Later, Madsley [2] carried out some modifications on the stability diagram for

cavability assessment [2]. However, the method suggested by Madsley [2] requires a large number of data from the earlier operations to increase the accuracy and precision of the analysis.

Some studies have adapted continuum modeling [16, 17], [19], where the simulation of discontinuity has been a significant challenge leading to the application of a more realistic discontinuous approach based on the Discrete Element Method (DEM). DEM is capable of characterizing rock mass cavability with a number of discontinuities such as the one conducted by Vakili and Hebblewhite [36]. In another study, the cavability of open-pit walls was investigated in the Palabora Mine [37].

In this study, the interaction of joint properties on cavability and quantitation of minimum caving span in terms of effective parameters on them were investigated, i.e. variables that had not been researched in the previous studies. In this study, a unique set of numerical simulations (480 models) was carried out using DEM to study the cavability of rock masses comprehensively. A series of artificial rock masses with a broad range of joint characteristics were prepared and tested to investigate the effects of joint set number (JN), joint spacing (JS), joint inclination angle (JI), joint surface friction angle (JF), and undercut depth (UD) (see Figure 1) on the cavability of rock mass. Response Surface Methodology (RSM) was employed to assess the interactive effects of defined independent variables (JN, JS, JI, JF, and UD) on the dependent variable, i.e. rock mass cavability, and finally, a polynomial model was proposed for measuring the cavability of rock mass based on the independent variables.

Though many researchers [10, 11, 22] have investigated the factors affecting the rock mass cavability, however, the main purpose of this paper is to obtain a) the statistical relationships of the effective parameters to compute the minimum required caving span in one hand, and b) to study the effect of the corresponding parameters interactions on rock mass cavability with a statistical approach.

In the previous studies, the expert opinions and empirical data have been used to investigate the effect of various parameters on cavability. Also in the previous studies, the range of changes in various parameters has been limited. In this study, the range of changes of each variable was much wider than the previous studies. Also in the previous studies, the statistical relationship for determining the minimum required caving span based on the affecting parameters the cavability has

not been presented, which has been done in this paper.

2. Methodology

In this work, in order to investigate the influence of discontinuity characteristics on the cavability of rock mass numerically, the following methodology was adopted. In the first step, the input parameters for numerical simulation including rock mass geotechnical parameters and joint characteristics were determined using the sensitivity analyses. In the next step, vast numbers of numerical models were created, and the model inputs were chosen based on the sensitivity analysis results, and rock mass cavability was evaluated accordingly. Finally, significant individual and interaction

influences of discontinuity and undercut parameters on rock mass cavability were calculated by employing a suitable series of statistical analyses.

2.1. Rock mass geo-technical parameters

The geo-technical properties of rock mass and discontinuities were chosen based on a variety of case studies conducted in this field [19]. The data was extracted from international caving Studies Report [19]. The list of parameters and their reasonable range are presented in Table 1. H indicates the height of the block from the top of the undercut to the ground surface, S indicates the joint spacing, and k is the ratio of horizontal to vertical stress.

Table 1. Value of fixed parameters to investigate effect of each solo parameter on minimum required undercut span.

Intact rock	Value	joints	Value	Parameter	Value
UCS (MPa)	130	Cohesion (MPa)	0	H (m)	500
Density (Kg/m ³)	2700	Friction angle (degrees)	30	K	1
Cohesion (MPa)	4.7	Normal stiffness (GPa/m)	2	S (m)	3
Friction angle (degree)	45	Shear stiffness (GPa/m)	0.2		

2.2. Numerical modeling

2.2.1. Model generation

Numerical simulation of rock mass caving has been investigated by many researchers [16-20]. It has been argued that three-dimensional modeling of block caving is impractical due to the run time and high amount of calculations ([8] and [36]). These problems have forced the researchers to apply 2D modeling approaches. Modeling in two dimensions can improve the calculation speed, and

more detailed geo-technical properties of rock mass can be used. Rock mass is a combination of intact rock and discontinuities. As a matter of fact, cavability of rock mass is affected by the discontinuity properties. Therefore, discrete element code (UDEC software) that can model discontinuities' properties was adopted to simulate rock mass. In this research work, rock mass was modeled with 350 m height and 1000 m length utilizing discrete element code (see Figure 1).

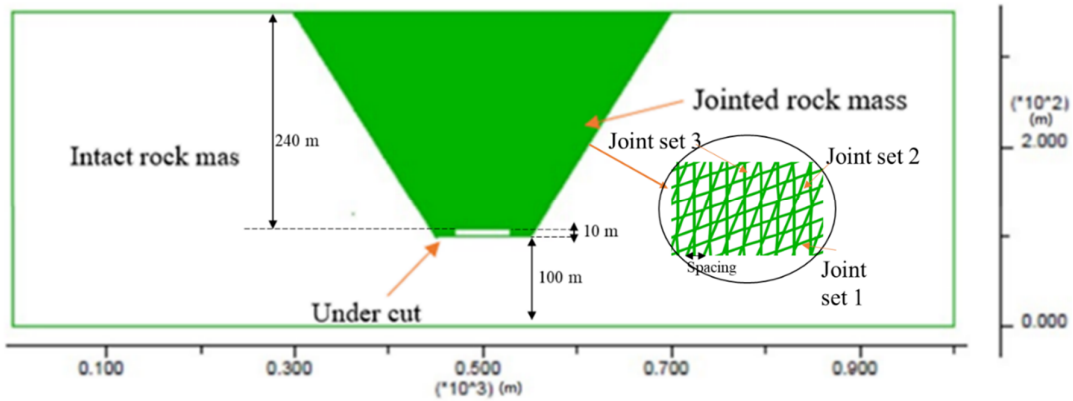


Figure 1. Numerical rock mass domain to model block caving.

For the purpose of saving time, the model was divided into jointed and un-jointed areas. The mesh

lengths in those two areas were 0.5 m and 10 m, respectively. The model was big enough to prevent

the effect of boundary condition on the caving process [39]. This type of mesh geometry and the used dimensions have already been utilized by Vyazmensky *et al.* [47] in the analysis of subsidence resulting from the block caving. This geometry is used to reduce computational time, which is similar to the results when the whole model is jointed. The model boundaries have been extended to avoid their effects on the results (4.5 times the maximum span created).

2.2.2. Numerical simulation process

In order to model rock mass caving, elastic model was first employed to solve the model and distribute uniform gravitational stress in the model domain. In the next step, the Mohr-Coulomb and

Coulomb Slip models were applied to the rock mass and discontinuities, respectively. Mainly three persistent and close joint sets with 20, 70, and 90 degree dip angles were added to the model. The undercut was extracted 2 m in length by 8 m in height at each step. This procedure was continued to reach the total span of 60 m where the caving occurred. In this model, out of the 200 m height of the waste and overburden, 40 m was modeled, and the rest was applied to the top of the model in terms of gravitational stress. A view of the model and its boundary condition is shown in Figure 1. The undercut (60 m × 8 m) was developed in stages in 2 m increments (in ore block), and the caved area was extracted continuously and regularly [39]. A view of the displacements at the first steps of simulation is presented in Figure 2.

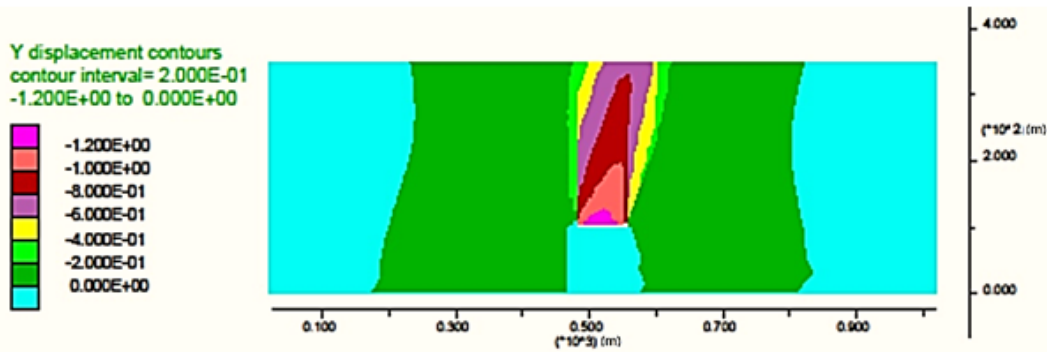


Figure 2. Displacement contours in the model with 60 m length undercut at first steps of solving before undercut.

After solving the model, all the blocks with displacements more than 1 m were labeled as the caved area [22]. For this purpose, the model was solved, and during the solution process, the blocks with displacements more than 1 m were removed to simulate regular and continuous extraction of the caved material. The extracted area and deformation zones in the numerical model are presented in Figure 3.

The minimum required caving span is the width of the undercut where the rock mass is caved. The

criterion used to find this span is displacement greater than 1 m. In other words, the width of the span increases sequentially with 2-m steps (in a constant geo-mechanical condition) until a displacement of 1 m is observed in the roof undercut. The span that causes a displacement of 1 m due to its creation is called the minimum required span. This criterion has already been introduced and validated by Sainsbury at the NorthPark Mine.

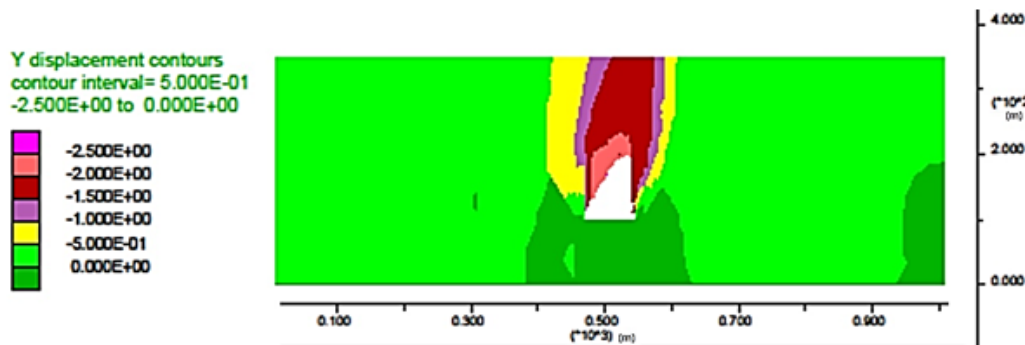


Figure 3. Final cavity and displacement contours around cavity.

3. Sensitivity analysis of effective parameters on rock mass cavability

In order to determine the most effective parameters on rock mass cavability, 283 models were created to investigate the effect of many parameters including gravitational stress, ratio of horizontal to vertical stress (K), compressive strength of intact rock, joint set numbers, joint cohesion, joint friction, joint spacing, and joint angle on the minimum required caving span (MRCS) to trigger caving initiation of rock mass. In each model, the effect of the solo parameter was studied, and the other parameters were kept constant at their presented value in Table 1.

In all models, vertical displacements more than 1 m of undercut roof were assigned as the caving criteria. The discontinuity properties were varied for all models, and undercut length was increased until caving was initiated. In this research work, based on the reports of a great many researchers, the effect of the main important parameters of rock mass including joint set number (JN), joint spacing (JS), joint inclination angle (JI), joint surface friction angle (JF), and undercut depth (UD) on cavability of rock mass were simulated. Therefore, sensitivity analyses were conducted based on the decision tree presented in Figure 4.

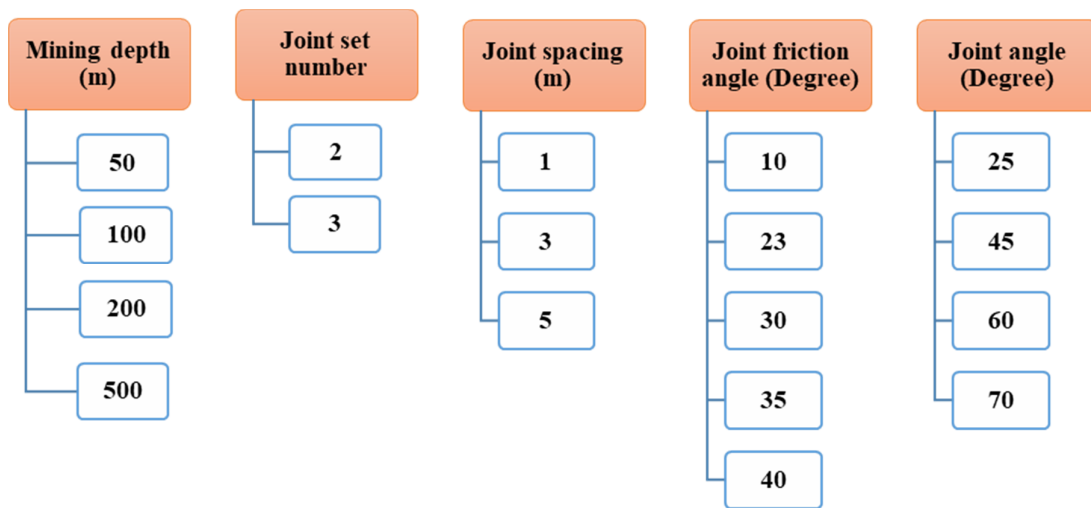


Figure 4. Possible modes for numerical experiments.

The effect of each parameter on rock mass caving was studied thoroughly, as can be seen in the following sections.

3.1. Effect of intact rock unconfined compressive strength

The effect of intact rock UCS was investigated using numerical models, and the results are presented in Figure 5. The results obtained indicate that in UCS below 100 MPa, by increasing unconfined compressive strength, MRCS increases dramatically, while in UCS more than 100 MPa, this parameter is not affected sharply by increasing UCS. The range of UCS was changed from 5 MPa

to 350 MPa. It was observed that in the range of 5 MPa to 100 MPa, with increasing the strength of intact rock, the rock mass became more stable, and the minimum required caving span increased. This means that in UCS, below 100 MPa, the mechanism of caving is failure in intact rock, and in UCS above 100 MPa, the mechanism of caving is slippage along the joints, and intact rock strength has no effect on the minimum caving span. This result is in high agreement with the reports of the researchers in the literature [18]. Therefore, UCS of intact rock was nominated as one of the influential parameters on rock mass cavability, and its range was chosen to vary from 5 MPa to 130 MPa.

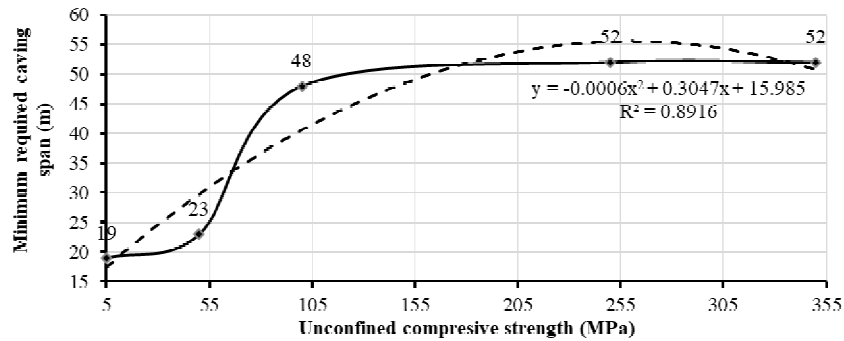


Figure 5. Effect of intact rock UCS on minimum required caving span.

3.2. Horizontal to vertical stress ratio

The ratio of horizontal to vertical stress (k) has a significant effect on the redistribution of induced stresses around the caved area, and it may dramatically affect failure development as well as the propagation of the rock mass. High value of this ratio can easily cause blockage of rock mass blocks and affect cavability of the rock mass. For this

purpose, the effect of ‘k’ ratio on MRCS was studied, and the result obtained is shown in Figure 6.

This figure indicates that an increase of ‘K’ ratio from 0.3 to 1.3 has a negligible effect on MRCS. This value increased from 34 m to 44 m by 29%. Moreover, the effect of ‘K’ ratio on the rock mass displacement was investigated, and the results obtained are illustrated in Figure 7.

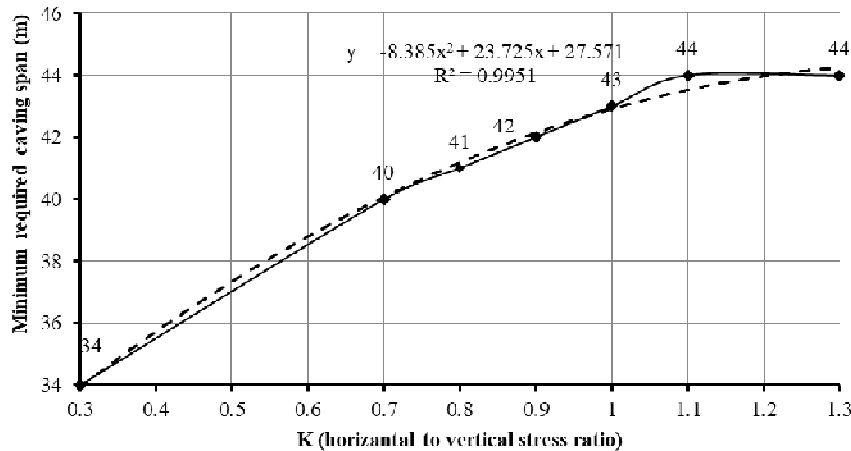


Figure 6. Effect of horizontal to vertical stress ratio on minimum required caving span.

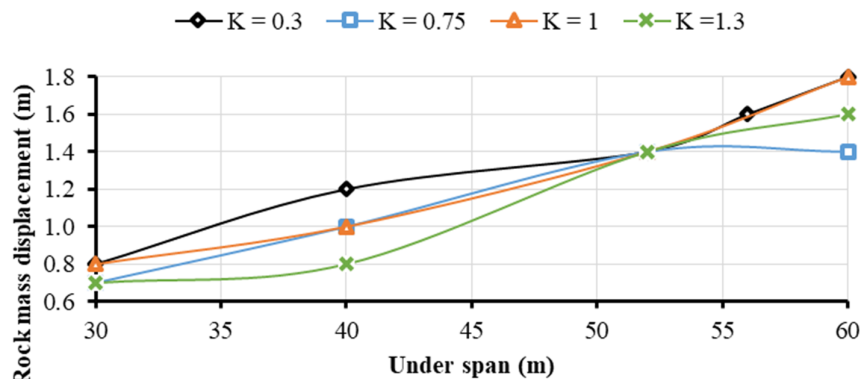


Figure 7. Effect of caving span on rock mass displacement in different k ratios.

The outcomes of simulations indicate that increasing 'k' ratio does not affect the displacements of the caving area significantly (Figure 7). On the other hand, the height of the caving area is developed by increasing the undercut span. According to these results, it can be concluded that the 'k' ratio does not affect cavability of rock mass significantly. Therefore, its value was decided to be constant at one.

In the models, the value of this parameter was changed from 0.3 to 1.3. It is observed that with increasing the value of K, the amount of displacement of the caving area in most of the spans does not change significantly (Figure 7). However, the modeling results show that the height of the caving area decreases with increasing K. In other words, a change in the value of K affects the propagation of the caving, and as it can be seen in Figure 6, has little effect on the span required to initiate the caving.

3.3 Undercut depth

Stress has the most significant effect on rock mass cavability. By increasing the ore depth, the

gravitational stress on ore body rises. In this paper, single individual effect of depth, i.e. gravitational stress was surveyed in 50, 200, 400, 600 and 800 m depths of undercut. In all models, 210 m of ore body was modeled, and overburden was applied on the top of the model in terms of the applied stress. The individual effect of undercut depth on MRCS is depicted in Figure 8. It can be seen from this picture that by increasing undercut depth, MRCS decreases.

From these diagrams it can be seen that, firstly, with increasing depth (increasing stress), the stability conditions become unfavorable and the minimum caving span for the beginning of caving decreases. Secondly, changes in this factor are more effective in medium to high friction angles. In other words, at low values of the joint friction angle, the depth has little effect on the minimum caving span. Comparing the results, we see that the rate of change is slower on slopes 45 and 60.

Figure 8 shows the results of a single-factor study (in which the undercut depth varies from 50 m to 800 m). Figures 9 to 12 show an example of the results of a multifactorial study (480 cases).

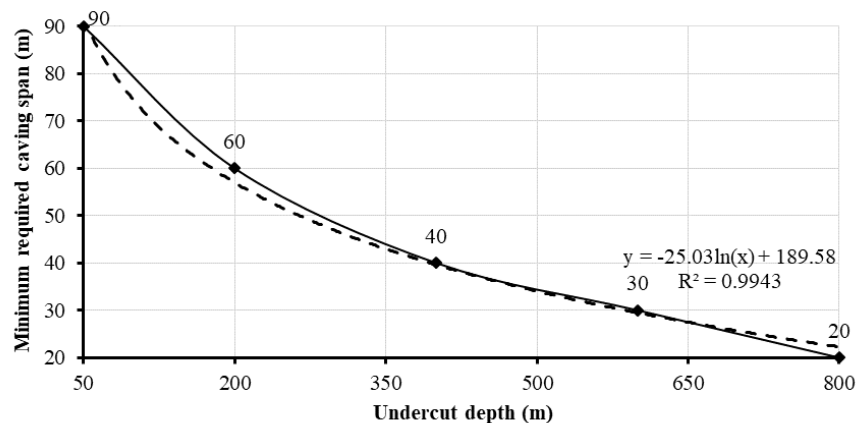


Figure 8. Effect of undercut depth on MRCS.

In addition, the effect of undercut depth in different joint dip angles as well as different joint surface frictions were studied. It is noteworthy that all models consisted of three joint sets with 2 m spacing. The joint angle varied in sizes of 25, 45,

60, and 70 degrees and the friction angle of the surface joint changed at sizes of 10, 23, 30, 35, and 40 degrees. The results of this analysis are illustrated in Figures 9, 10, 11, and 12.

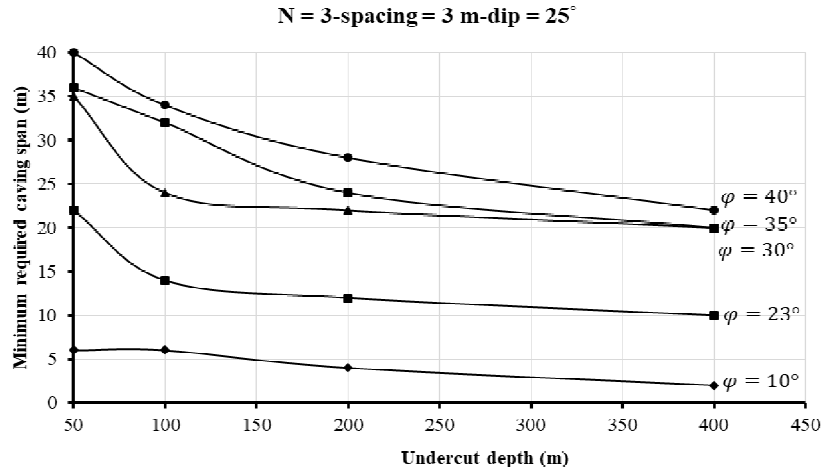


Figure 9. Effect of undercut depth on MRCS in joint inclination of 25 degrees and in different joint friction angles.

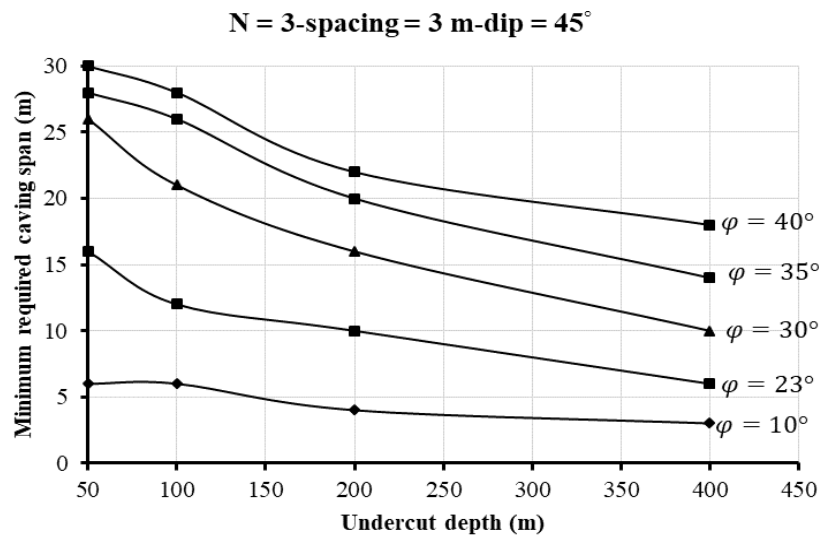


Figure 10. Effect of undercut depth on MRCS in joint inclination of 45 degrees and in different joint friction angles.

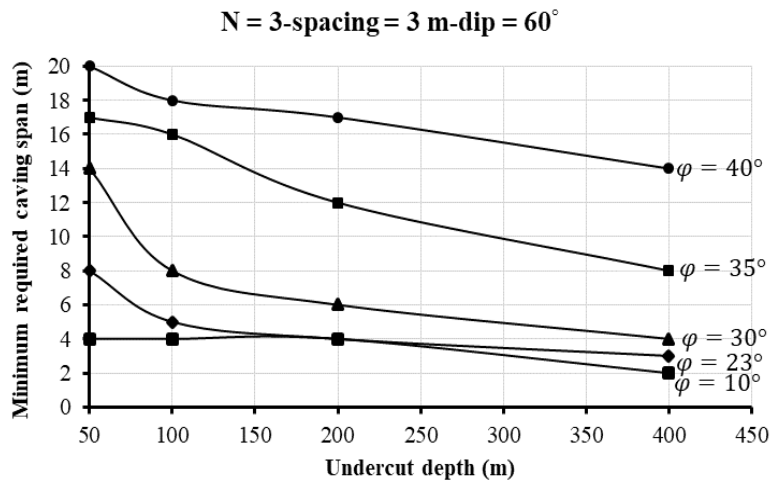


Figure 11. Effect of undercut depth on MRCS in joint inclination of 60 degrees and in different joint friction angles.

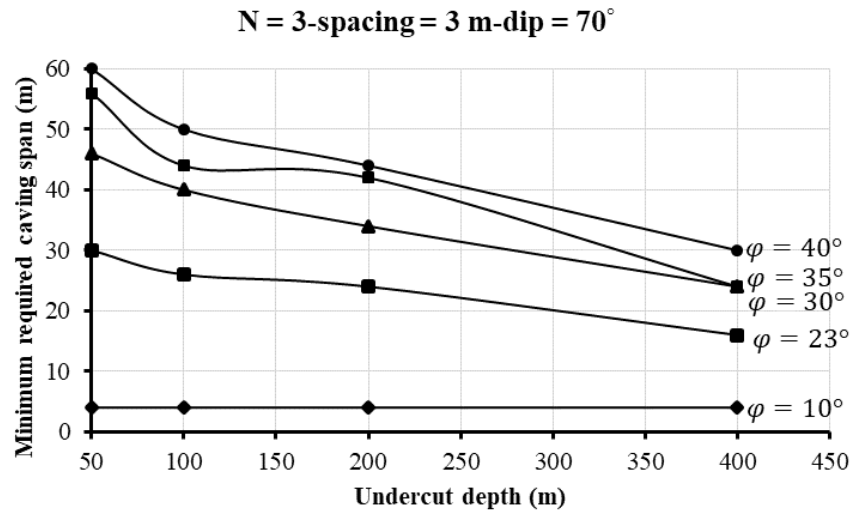


Figure 12. The effect of undercut depth on MRCS in joint inclination of 70 degrees and in different joint friction angles.

According to the figures presented, it can be inferred that by increasing the undercut depth, MRCS decreases significantly. Furthermore, it should be noted that the effect of undercut depth on MRCS is more than the mean values of the joint friction angle. In other words, at low levels of joint friction, undercut depth does not affect MRCS. By comparing the figures, it can be seen that the incremental rate of MRCS at joint angles of 45 and 60 degrees is the lowest one.

3.4. Joint spacing

Joint spacing has a significant effect on rock mass cavability. Deformation and fracture

mechanism of a rock mass vary with the ratio of spacing to caving span dimension. The effect of joint spacing on minimum required caving span was investigated, and the results are presented in Figure 13. As it can be seen in this figure, by increasing the joint spacing, the minimum required caving span increases.

As the joint spacing increases, the created blocks become larger, and more force is required to move them. Therefore, the minimum required caving span increases.

The effect of ore body depth on rock mass cavability with three joint set numbers in different joint friction angles are presented in Figure 14.

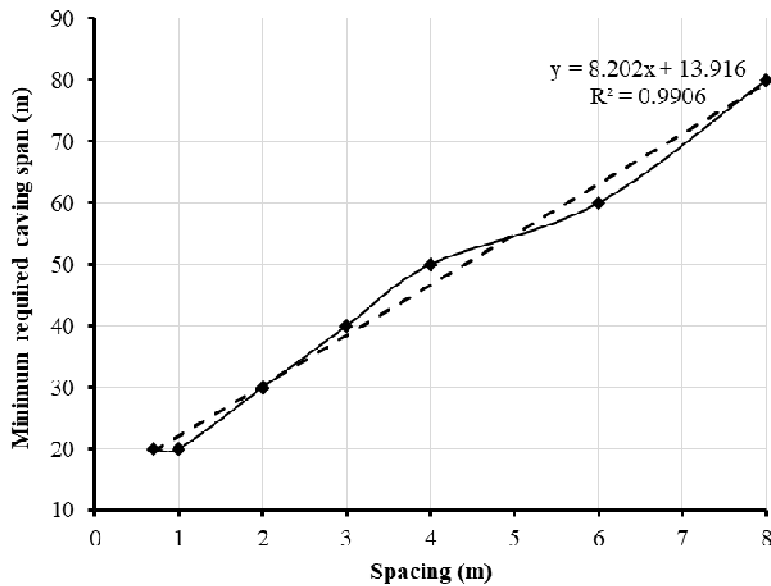


Figure 13. Effect of joint spacing on MRCS.

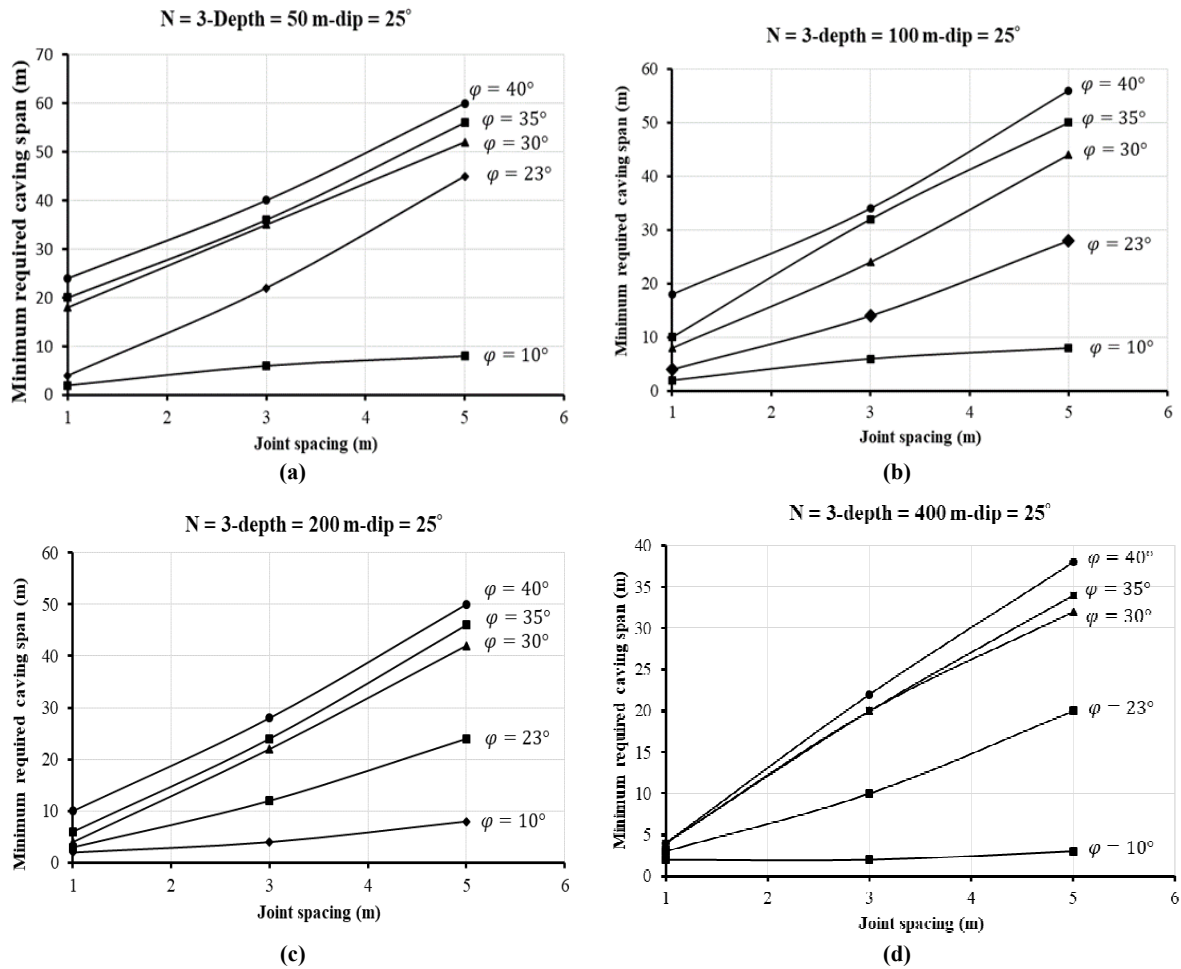


Figure 14. Effect of joint set on MRCS of rock mass with three joint sets at different joint friction angles a) Ore body depth 50 m b) Ore body depth 100 m c) Ore body depth 200 m d) Ore body depth 400 m.

It can be inferred from Figure 14 that by increasing joint spacing, stability conditions worsen and MRCS increases. It should be noted that at low levels of joint friction, the variation of joint spacing does not affect MRCS; in other words, joint friction has a higher effect on MRCS (Figure 14a). It can be inferred from Figure 14 that by increasing the joint friction angle, the variation rate of MRCS also rises (Figure 14a, b, c, and d). In addition, at intermediate spacing and high joint spacing, the MRCS for all depths is almost the same (Figure 14a, b, c, and d). At low spacing of joints, the MRCS has minimum variation. In addition, at low joint spacing, by increasing the depth, the MRCS rates at different joint friction angles are close to each other.

3.5. Joint friction angle

The effect of joint angle on MRCS was investigated using numerical modeling. For this purpose, all parameters were kept constant at their

average (Table 1) and the joint angle varied from 5 to 45 degrees. As it can be seen in Figure 15, from the joint friction angle of 5 degrees to the joint friction angle of 30 degrees, MRCS increases with mounting rate, and after the joint friction angle of 30 degrees, the joint angle does not affect MRCS significantly. It can be inferred from Figure 16a that at lower than the joint friction angle of 30 degrees, MRCS rises with mounting rate, and after this angle, the increment rate decreases dramatically. Furthermore, it can be seen that by increasing ore body depth, MRCS climbs. The effect of joint dip angle is presented in Figure 16b, where it can be seen that MRCS at joint friction angle of 10 degrees is not affected by joint angle, and it is the same for all the joint inclinations. Moreover, as joint inclination climbs from 15 degrees to 60 degrees, MRCS drops gradually. In contrast, MRCS rises from joint friction angle of 5 to that of 35 degrees linearly, and after that the increment rate decreases. The effect of joint spacing and friction angle on

MRCS is depicted in Figure 16c. It can be inferred from this figure that by increasing joint spacing, MRCS rises gradually, and in higher joint friction spacing, it affects MRCS more than lower joint spacing. The effect of joint friction on different joint set numbers is illustrated in Figure 16d. In this figure, it can be seen that by increasing joint set number and joint friction, the MRCS decreases dramatically.

The modeling results showed that at low friction angles, the most effective parameter was the

friction angle, and other parameters had very little effect. This is because at low friction angles, the joints have very little shear strength, which moves due to very low force (even very shallow depths and low stresses) and caving initiate. The higher the friction angle of the joint surface, the higher the shear strength of the joints, and as a result, more force will be required to slip. Thus the minimum required caving span increases with increasing friction angle (Figure 15).

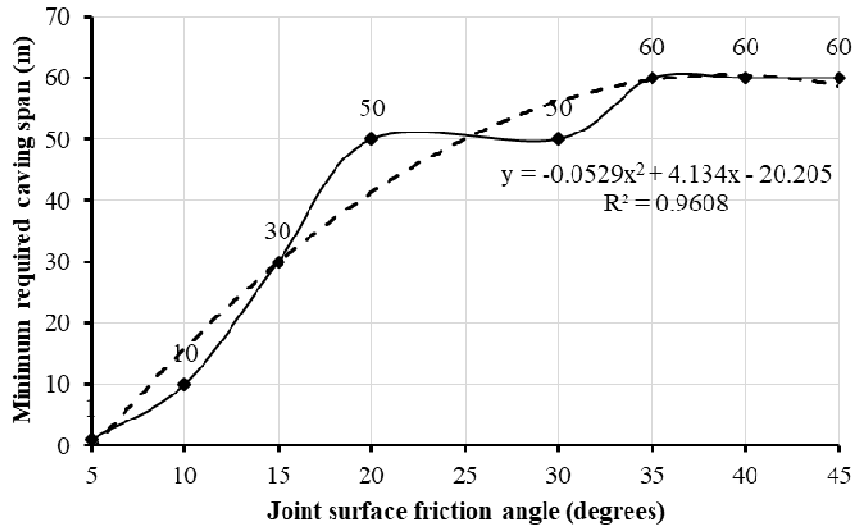


Figure 15. Effect of joint friction on MRCS of rock mass with three joint sets and depth of 500 m at different joint friction angles.

3.6. Joint cohesion

The impact of joint cohesion on MRCS was investigated, and the results obtained are presented in Figures 17 and 18. As illustrated in Figure 17, joint cohesion does not affect MRCS.

One of the parameters affecting the caving is the shear strength of the joints. Shear strength is affected by two factors: cohesion and friction angle. Therefore, with the increase of each one of

these parameters, the shear strength increases, and as a result, the minimum caving span increases. However, the point is that according to library studies, the range of cohesion of joints in mines is between zero (for diorite, granodiorite and porphyry fillers) and 0.36 MPa (for montmorionite filler). The modeling results in this interval showed that cohesion had no effect on the minimum caving span. For values greater than 0.4 MPa, cohesion is likely to affect caving.

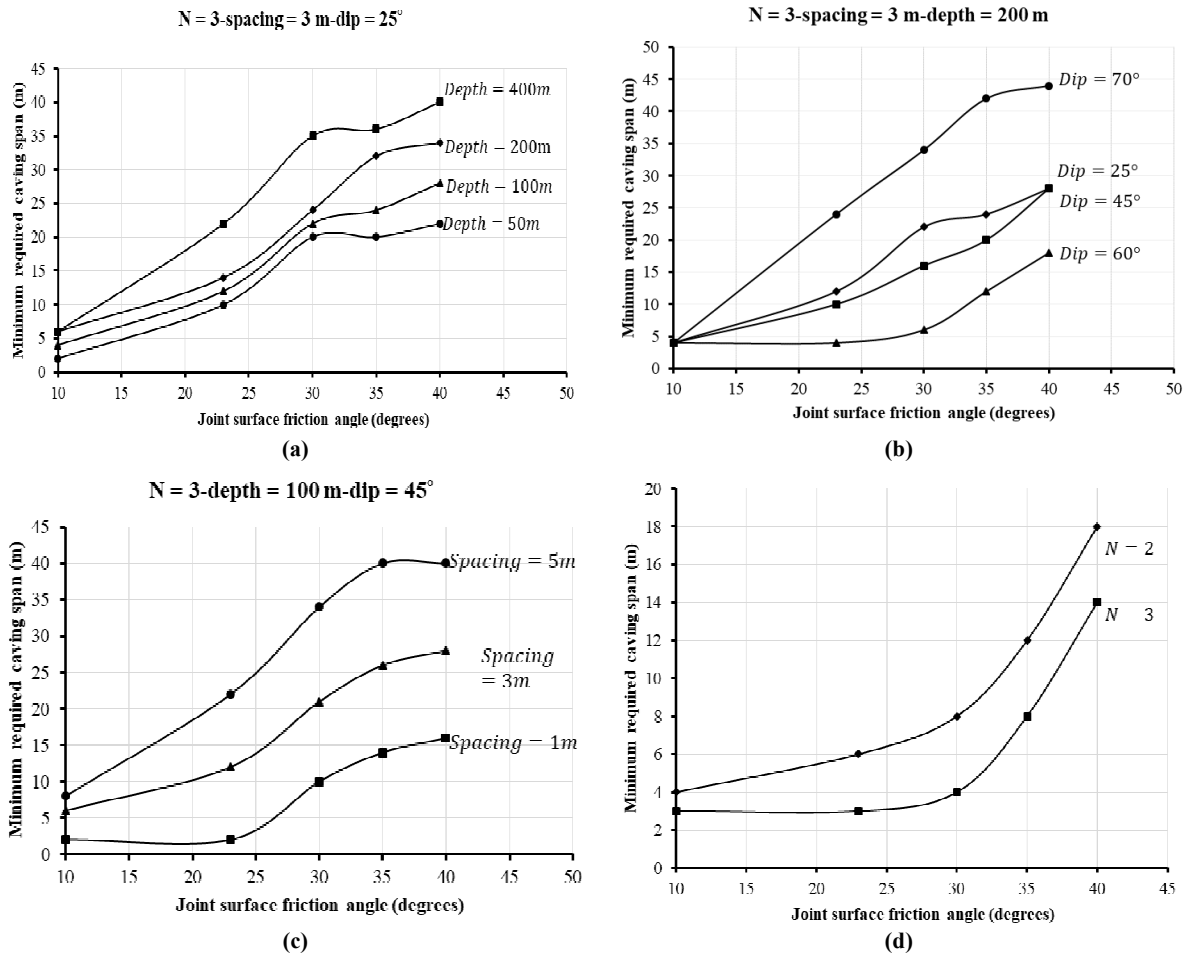


Figure 16. Effect of joint friction angle on MRCS when a) Ore body depth varies and there are three joint sets with average spacing of 3 m and joint dip of 25 degrees, while ore body depth is 50 m b) Joint angle varies and there are three joint sets with average spacing of 3 m and ore body depth of 200 m c) Joint spacing varies and there are three joint sets with the joint dip of 45 degrees and ore body depth of 100 m d) Joint set number varies and joint dip and spacing are 60 degrees and 3 m, respectively, and ore body depth is 400 m.

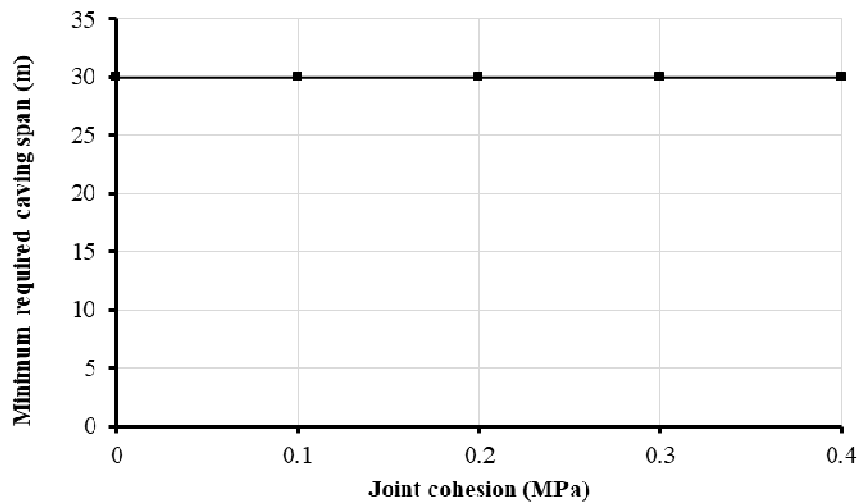


Figure 17. Effect of joint cohesion on MRCS of rock mass with three joint sets with average spacing of 3 m and joint sets 1, 2, and 3 are 45, 135, and 90 degrees, respectively. The rest of the parameters are similar to the results shown in Table 1.

Moreover, the effect of joint cohesion on rock mass displacement in different caving spans was investigated, and the results obtained are presented in Figure 18. It can be seen that in the same span,

the variation of joint cohesion does not affect MRCS. It can be inferred that cohesion has a neutral influence on MRCS.

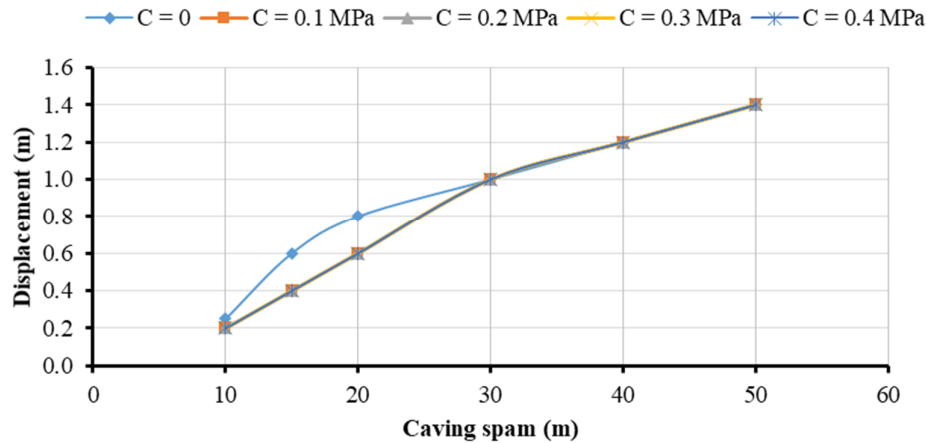


Figure 18. Effect of joint cohesion on rock mass displacement in different caving spans.

3.7. Joint inclination angle

The effect of joint dip angle along with joint friction angle, ore body depth, joint spacing, and joint set number was investigated numerically. Owing to the complexity of joint inclination and its effect on rock mass cavability, two possibilities of joint configuration were studied first. At the first step, one joint was considered to be horizontal and the two other joints to be conjugates. The result of rock mass cavability analysis in this joint configuration is illustrated in Fig 19a. The second possibility is that the first joint is vertical and the two other joints are conjugate. The outcomes of rock mass cavability containing this joint configuration are depicted in Figure 19b. As it can be seen in Figures 19a and 19b, MRCS is minimal at the conjugated joint angle of 60 degrees. It can be inferred that MRCS is highly affected by rock mass anisotropy. By making a comparison between Figures 19a and 19b, it can be inferred that when the third joint is horizontal, MRCS is much less than the vertical one.

The effects of joint friction angle, ore body depth, spacing and joint set number along with joint inclination on rock mass cavability were investigated numerically, and the results are presented in Figure 20. It can be inferred from Figures 20a, b, c, and d that by increasing the conjugate joint dip angle from 25 to 60 degrees, MRCS decreases and reaches its minimum at 60 degrees and after that it increases by increase in the conjugate joint angle. The main reasons for this are decrease in the required stress for caving by

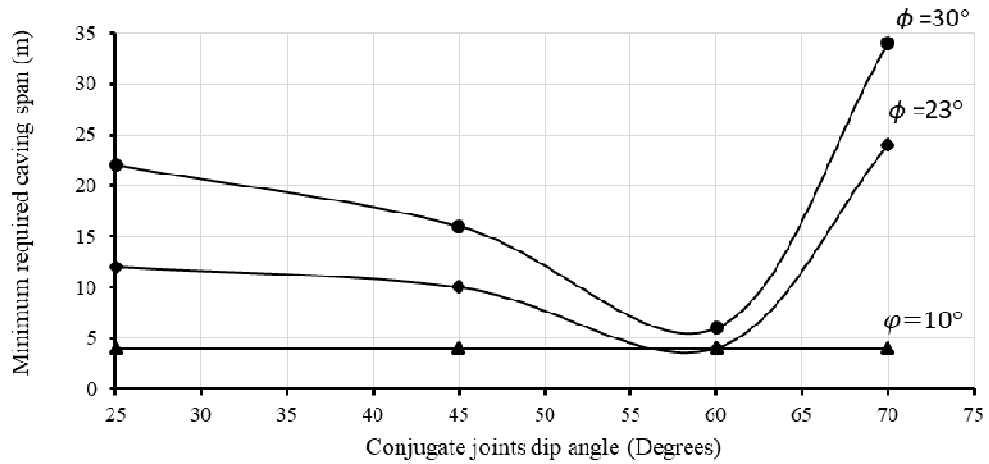
reducing the angle between the joints and the maximum principal stress, the ratio of sine component of gravitational force to its cosine component, and the spread of the area with caving potential [19]. When the joint angle is 25 degrees, the two first factors affect rock mass cavability positively, and result in the reduction of MRCS. In this situation, the angle between maximum principal stress joint inclinations is 65 degrees. With this angle, a higher amount of stress is required for the failure to occur. On the other hand, when the inclination of joint sets is 25 degrees, the driven force (sine component) is less than the resistant force (cosine component).

At the joint angle of 45 degrees, the two factors of reducing the angle between the joints and the maximum principal stress and the spread of the area with caving potential have positive effects on the failure process. Therefore, the maximum required stress for caving at the joint angle of 45 degrees is less than the joint angle of 25 degrees. In contrast, the area of rock mass with failure potential at the 45-degree joint angle is more than that of the 25 degree joint angle. At the joint angle of 60 degrees, all the three above-mentioned factors positively affect the failure process. In this case, the 30-degree angle between the maximum principle stress and the joint inclination reduces the required stress for the failure process in comparison to the 25 and 45 degree joint angles. The main reasons for this are decrease in the required stress for caving by lowering the angle between the joints and the maximum principle stress, the ratio of sine component of gravitational

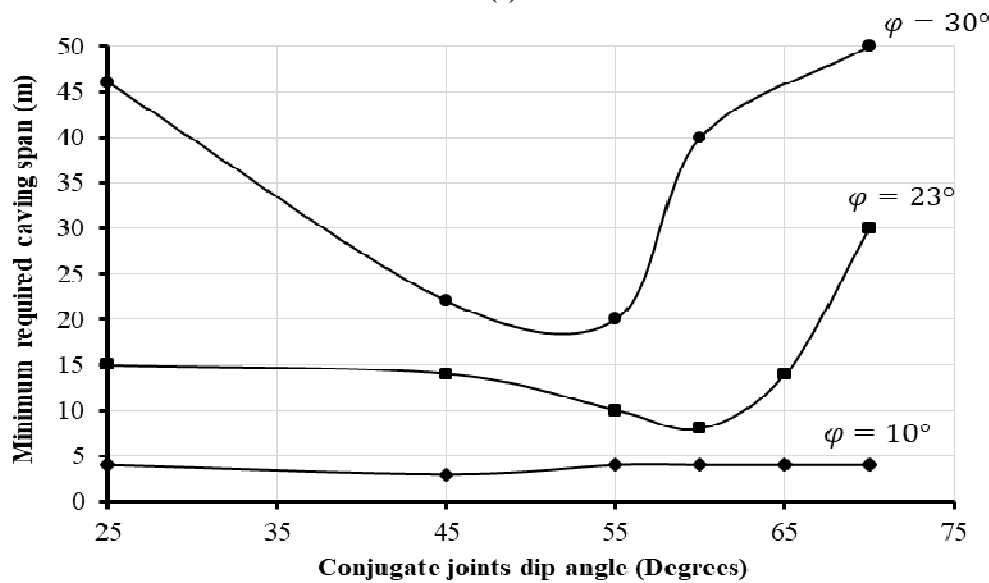
force to its cosine component, and the spread of the area with caving potential. What is more, the driving force (sine component) is much more than resistant force (cosine component).

In the case of a 70-degree angle, less area of rock mass is exposed to the failure process but the driving force is much more than the resistant one. Therefore, in this joint angle, more stress is required for rock mass failure than the 60 degree joint angle, and rock mass failure is more

controlled by the joint friction angle. Rock mass with joint inclinations of 25 and 70 degrees is much more affected by joint spacing, in which interlocking of blocks reduces roof displacement, so MRCS increases. MRCS increases by omitting horizontal bedding of rock mass. The results of this work revealed that the variation of MRCS compared to the joint angle was U-shaped and reached a minimum at the joint angle of 60 degrees.



(a)



(b)

Figure 19. Effect of joint inclination on MRCS in different joint friction angles and depth of 200 m when a) joint set is horizontal and there are two other conjugates, b) joint set is vertical and there are two other conjugates.

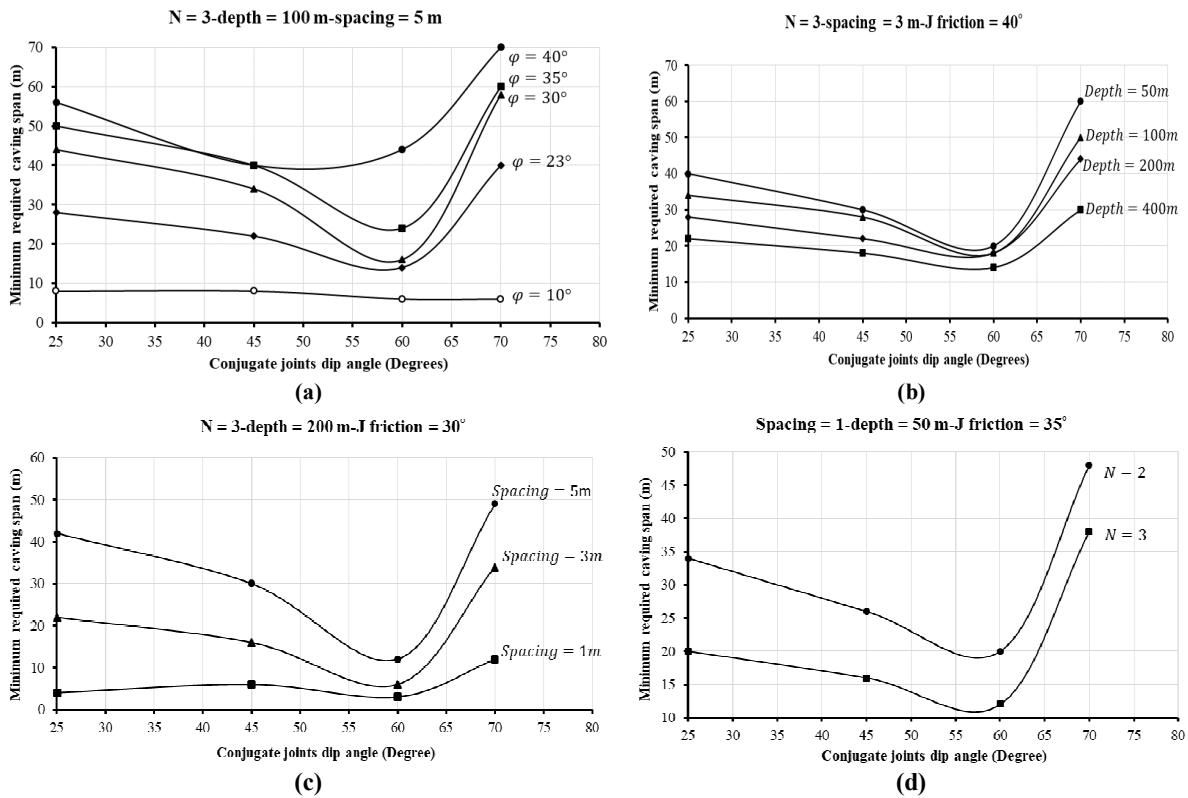


Figure 20. Effect of joint inclination angle on MRCS when a) joint inclination varies and there are three joint sets with average spacing of 5 m and ore body depth of 100 m b) ore body depth varies and there are three joint sets with the average spacing of 3 m and joint friction angle of 40 degrees c) joint spacing varies and there are three joint sets with the joint dip of 30 degrees and ore body depth of 200 m d) joint set number varies and joint friction angle and spacing are 35 degrees and 1 m, respectively, and ore body depth is 50 m.

3.8. Joint set number

The impact of joint set number along with joint spacing and ore body depth on rock mass cavability was investigated, and the results are presented in Figure 21. It can be inferred from Figure 21a, b, and c that by increasing the joint set number, MRCS decreases. It can be seen that at a constant span, failure shape and its spread are completely different (Figure 21).

As the number of joint sets increases, the dimensions of the created blocks become smaller and the environment is created with more

fragmentation, which results in unfavorable stability conditions and more instability. As a result, increasing the number of joint sets increases the chance of caving and reduces the minimum required caving span. The slope of the changes of the minimum caving span from 1 to 3 is very sharp, and from the number of joint set 3 onwards is very low.

It means that failure zone shape depends on joint set numbers and their dip angles. Furthermore, variation of joint set number at low levels of joint spacing does not affect MRCS (Figure 22).

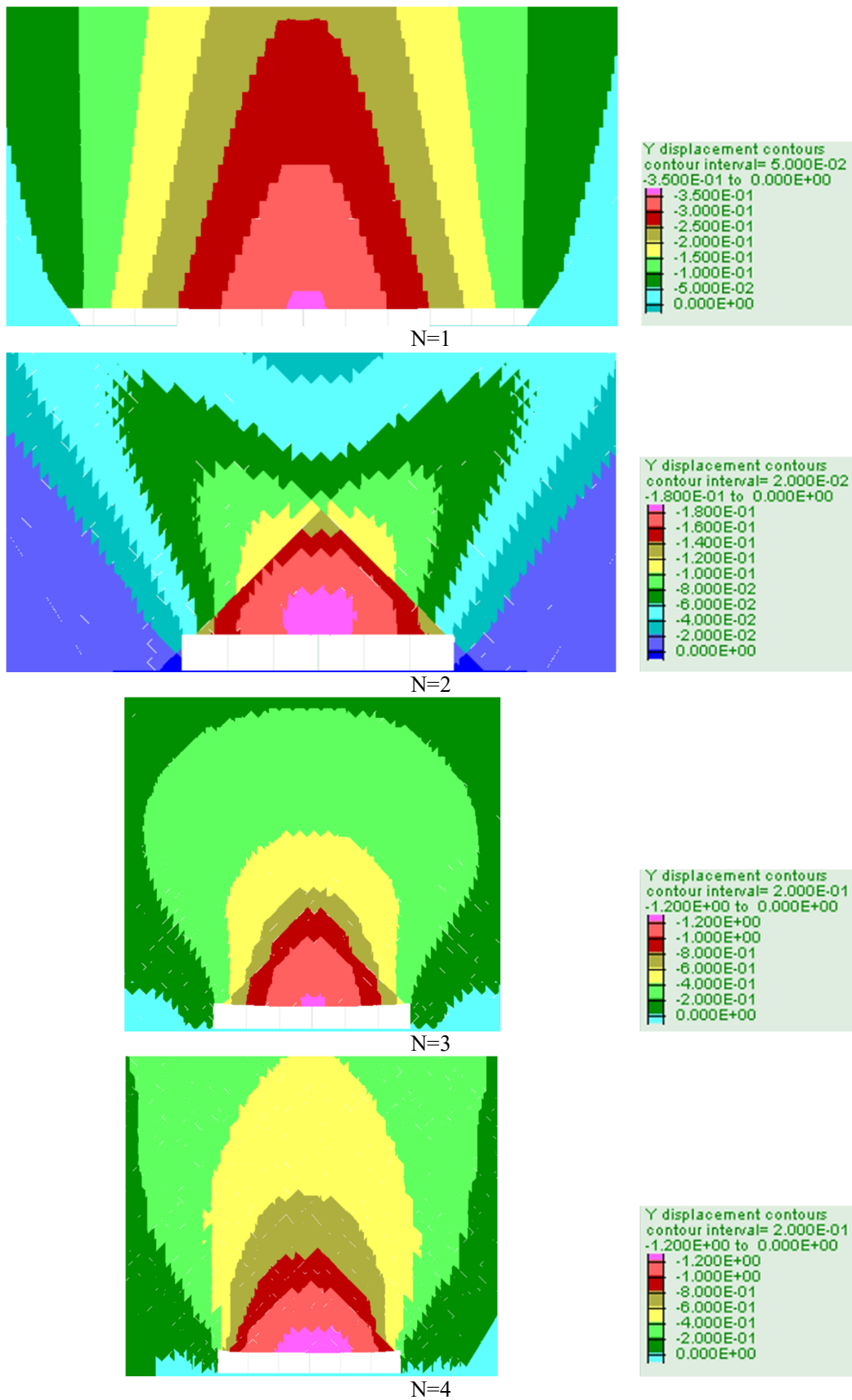
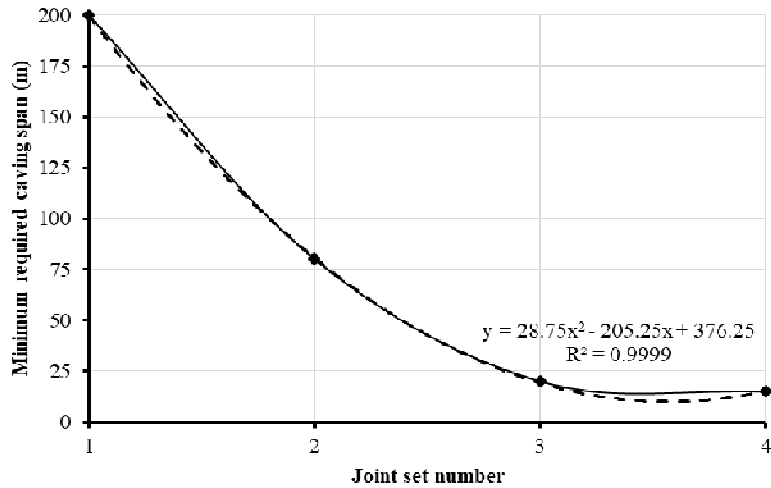
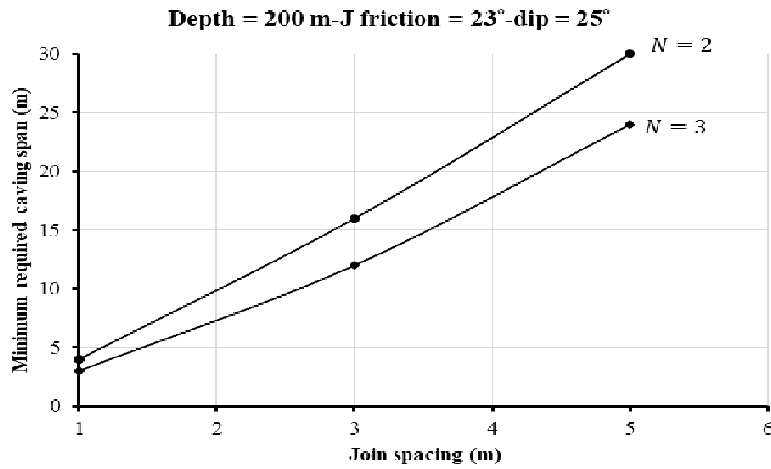


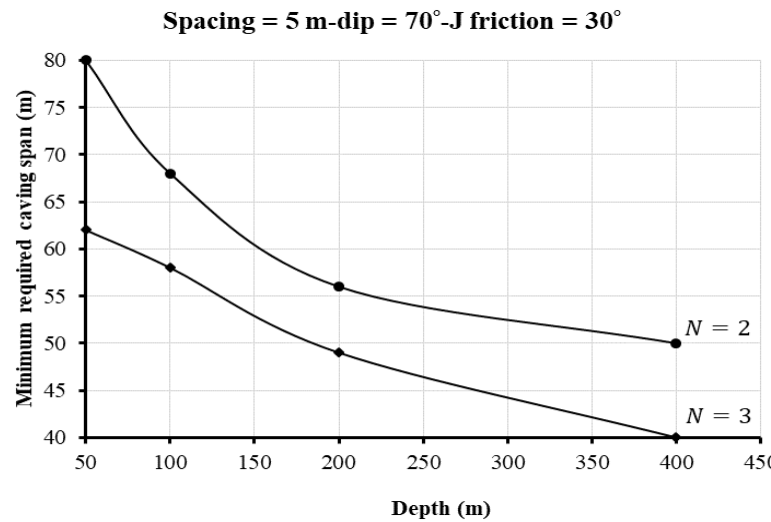
Figure 21. Effect of joint set number on failure zone shape.



(a)



(b)



(c)

Figure 22. Effect of joint set number angle, spacing, and ore body depth on MRCS when a) just the joint set number varies b) the effect of joint spacing in different joint set numbers while joint friction angle and dip are 30 and 70 degrees, respectively, and the ore body depth is 200 m c) ore body depth varies while joint friction angle and spacing are 30 degrees and 5 m, respectively, and joint inclination is 70 degrees.

4. RSM modeling

In order to study the effect of rock mass geo-mechanical and geometrical properties on its cavability, the effect of joint set numbers, joint spacing, joint inclination angle, joint surface friction angle, and the depth of undercut on minimum caving span were investigated statistically. Therefore, for further understanding of the relationship between MRCS and the rock mass parameters, historical design of Response Surface Methodology (RSM) was adopted to investigate the coupled influences of the rock mass properties on the response.

4.1 Design of experiments and RSM

The design of experiments (DOEs) methods, like RSM, which are based on the statistical and arithmetical approaches, was developed to model a process and explain the interaction of factors on the response of a system [40-47]. RSM is able to deal with a few number of experiments to investigate the interaction amongst variables and their influence on the response [38]. In this paper, a mathematical model was developed utilizing the

Design-Expert 7 software, and historical data design was utilized to model RSM. The independent variables included in the modeling process were joint set numbers (JN), joint spacing (JC), joint inclination angle (JI), joint surface friction angle (JP), and depth of undercut (DU) (Figure 6). The dependent variable is the MRCS, which can be expressed using a quadratic model as follows ([40], [41], [45], [47]).

$$y = \beta_0 + \sum_{i=1}^3 \beta_i X_i + \sum_{i=1}^3 \beta_{ii} X_i^2 + \sum_{i=1}^3 \sum_{j=i+1}^3 \beta_{ij} X_i X_j \quad (1)$$

where y is the response variable representing the minimum caving span of rock mass; β_{ii} , β_{ij} , β_i , and β_0 are regression coefficients; and X_i and X_j are the values of the independent variables coded in the program and can be expressed as follows:

$$X_i = \frac{x_i - x_0}{\Delta x} \quad (2)$$

where x_0 is the value of x_i at the center point and Δx is the change step. The code and level of the independent variables are presented in Table 2.

Table 2. Independent variable codes and their levels in historical data design of experiments.

Factor	Code	Level	
		-1	1
Joint set number	JN	2.00	3.00
Joint spacing (m)	JS	1.00	5.00
Joint inclination angle (degrees)	JI	25.00	70.00
Joint surface friction angle (degrees)	JF	10.00	40.00
Depth of undercut	UD	50.00	400.00

4.2 Variance Analysis (ANOVA)

The analysis of variance (ANOVA) technique was adopted to estimate the contribution of each

parameter and their coupled effect on the response [40]. The statistical properties of the proposed model are shown in Table 3.

Table 3. Statistical parameters of RSM models.

Statistical parameter	Model	Description
F-value	288.18	Model is significant
Adequate precision	74.087	Model can be used to navigate the design space
R2	0.8642	High correlation between the exponential and the predicted values
Adjusted-R2	0.8604	In a good agreement with their R2 coefficient

Based on Table 3, the F-value of the model indicates its significance. There is only a 0.01% chance that such a large "Models F-Value" occurs due to noise. The "Adequate Precision" measures

the signal-to-noise ratio. A ratio greater than 4 is desirable.

In addition, the actual and predicted minimum caving span is illustrated in Figure 23, and shows a linear regression relationship.

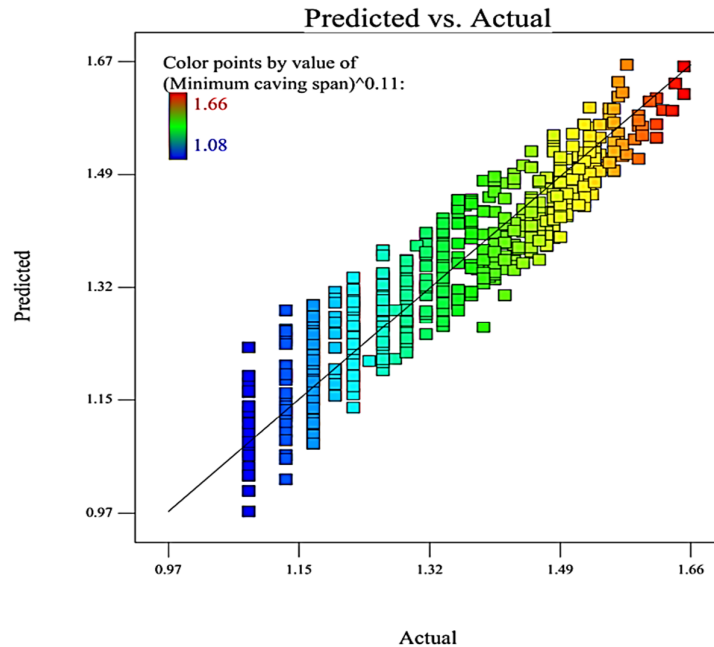


Figure 23. Actual and predicted minimum caving span of block caving models.

Response transformation is a crucial component of any data analysis. Transformation is necessary if the error (residuals) is a function of the value of the response. The normality is usually checked by normal plot of the residuals. When there is a pattern in the plot of residuals versus predicted response values, response transformation is necessary. Unless the ratio of the maximum response to the

minimum response is large, transforming the response will not make much difference [48]. The relationship between the normal percentage probability and the standardized residual of the model is depicted in Figure 24. As it can be seen, there is a linear pattern between standardized residuals versus predicted response values. Therefore, response transformation is vital.

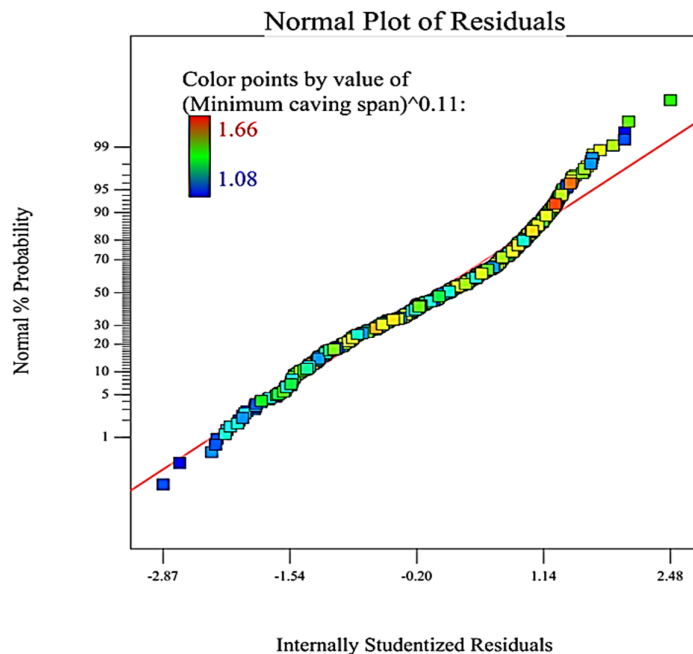


Figure 24. Normal probability plot for minimum caving span of block caving models.

Therefore, Box-Cox plot (See Figure 25) provides a recommended transformation from the power family as follows:

$$MRCS_{transformed} = (MRCS_{Untransformed})^{Lambda}, Lambda = 0.11 \quad (3)$$

$$MRCS^{0.11} = 1.37365 - 0.049361 \times JN - 0.00055UD + 0.077417JS + 0.012689JF - 0.015113JI + 0.0000298UD \times JS - 0.0000057UD \times JF + .000396JS \times JF - 0.000475JS \times JI + 0.000000703UD^2 - 0.00426JS^2 - 0.0000773JF^2 + 0.000183JI^2 \quad (3)$$

$$MRCS^{0.11} = 1.27 - .025 \times JN - 0.051UD + 0.091JS + 0.13JF + 0.02JI + 0.01UD \times JS - .015UD \times JF + 0.012JS \times JF - .021JS \times JI + 0.022UD^2 - 0.017JS^2 - 0.017JF^2 + 0.017JI^2 \quad (4)$$

The effect of each individual parameter and their mutual effect on MRCS were investigated by

means of ANOVA, and the results are presented in Table 4.

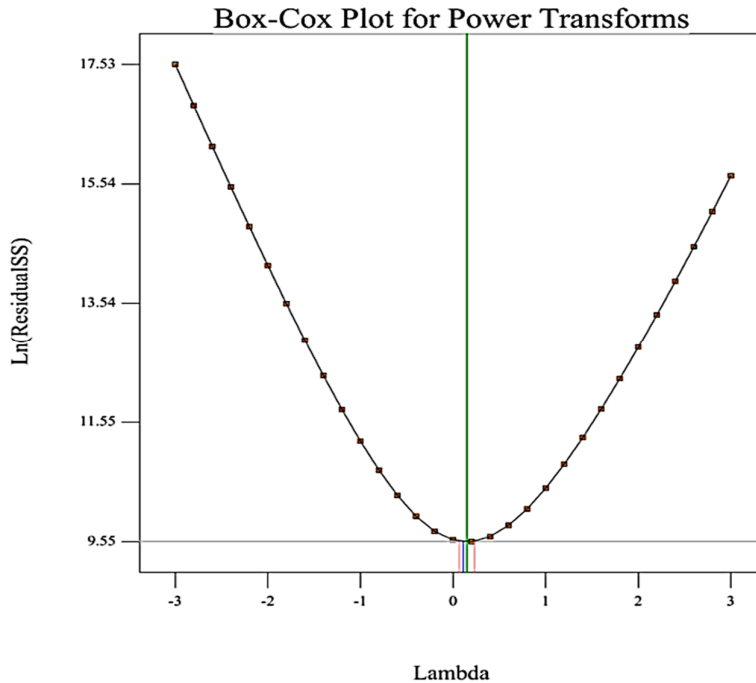


Figure 25. Box-Cox plot recommends a power transformation with Lambda = 0.11.

ANOVA indicates that all parameters that were chosen in Section 3 to investigate cavability of rock mass highly affect MRCS. In other words, the results of ANOVA are in high agreement with the results of conventional sensitivity analysis. Moreover, a combination of joint spacing and joint inclination has the highest mutual effect on MRCS, and a combination of undercut depth and joint spacing has the lowest effect on MRCS.

4.4 Effects of rock mass parameters on MRCS
4.4.1 Individual effect of rock mass parameters on MRCS

The influence of each independent variable, i.e. joint set number, undercut depth, joint friction, joint spacing, and joint inclination on MRCS is illustrated in Figure 26, in terms of their coded values. According to Figure 26, an increase in the joint set number from 1 to 3 decreases MRCS from 10.47 m to 7.35 m by 29.77%. In addition, increasing undercut depth from 50 m to 400 m causes a 50.94% decrease in MRCS (from 14.52 m to 7.12 m). However, with an increase in joint

spacing from 1 m to 5 m, MRCS rises from 3.09 m to 14.75 by 376.73%. It is noticeable that an increase of joint friction from 10° to 40° leads to an increase of 638.70% in MRCS (from 2.58 m to

19.10 m). Finally, as it is depicted in Figure 24, the variation of MRCS versus joint inclination (from 25 to 70 degrees) is non-linear, showing a minimum at 45 degrees.

Table 4. ANOVA of RSM modeling for dependent parameters.

Parameters	Sum of squares	df	Mean square	F-Value	Weighting contribution (%)	P-value
Model	8.872	13	0.682	228.183	7.819	< 0.0001
JN	0.292	1	0.292	97.757	3.348	< 0.0001
UD	0.665	1	0.665	222.369	7.624	< 0.0001
JS	2.303	1	2.303	769.990	26.404	< 0.0001
JF	3.651	1	3.651	1220.774	41.860	< 0.0001
JI	0.109	1	0.109	36.572	1.250	< 0.0001
UD × JS	0.020	1	0.020	6.844	0.229	0.0092
UD × JF	0.031	1	0.031	10.422	0.355	0.0013
JS × JF	0.021	1	0.021	7.062	0.241	0.0081
JS × JI	0.083	1	0.083	27.810	0.952	< 0.0001
UD ²	0.036	1	0.036	12.010	0.413	0.0006
JS ²	0.031	1	0.031	10.346	0.355	0.0014
JF ²	0.026	1	0.026	8.537	0.298	0.0036
JI ²	0.772	1	0.772	258.027	8.851	
Residual	1.394	466	0.003			
Cor total	10.266	479				

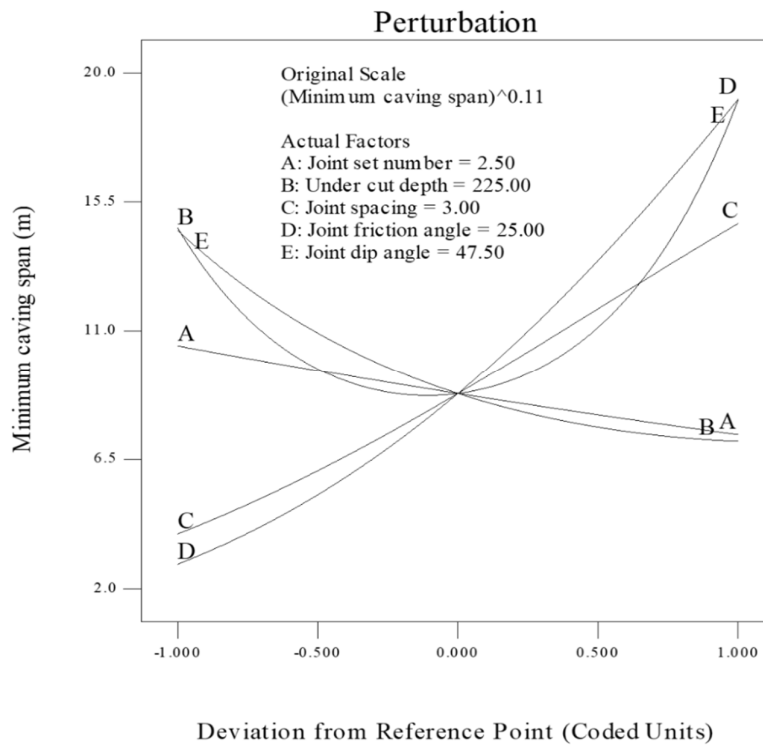


Figure 26. Individual effects of each independent parameter on minimum required undercut length.

4.4.2. Mutual effects of rock mass parameters on MRCS

Figure 27a shows the influence of joint spacing number and undercut depth on MRCS. As it can be seen, while undercut depth is constant, an increase in the joint spacing number has a negative effect on

MRCS. It is important to note that when the undercut length is 50 m, an increase in joint spacing from 1 to 5 causes 204.30% increase in MRCS (from 7.28 m to 22.17 m); however, when undercut depth is 400 m, a 355.83% increase is caused by raising joint spacing. Furthermore, when joint spacing is constant and is 1 m, an increase in

undercut depth from 50 m to 400 m causes a 60.86% decrease in MRCS (from 7.29 m to 2.85 m), and when joint spacing is 5 m, MRCS decreases by 41.38% (from 22.17 m to 13.00 m).

Figure 27b shows the effect of joint friction and undercut depth on MRCS. According to this figure, while joint friction is constant, an increase in the undercut depth has a negative effect on MRCS. It is important to note that when joint friction = 10° , an increase in undercut depth from 50 m to 400 m causes a 43.08% decrease in MRCS (from 4.47 m to 2.54 m); while joint friction = 40° , this increase in undercut depth causes 57.28% decrease in MRCS (33.27 m-14.21 m). Moreover, as it is shown in Figure 25b, while the undercut depth is constant, an increase in joint friction increases MRCS. When undercut depth = 50 m, an increase in the joint friction from 10° to 40° causes a 643.42% increase in MRCS (from 4.47 m to 33.27 m); and when undercut depth = 400 m, this increase in joint friction causes a 457.94% increase in the MRCS (from 2.56 m to 14.21 m).

Figure 27c shows the influence of joint spacing and undercut depth on MRCS with keeping the other parameters constant at their middle levels. According to Figure 25c, while the joint friction angle is constant, an increase in the joint spacing has a positive effect on MRCS. It is important to note that when joint friction angle = 10° , an increase in the joint spacing from 1 m to 5 m causes a 272.36% increase in MRCS (from 1.27 m to 4.67 m); however, when joint friction angle = 40° , a 295.50% increase is caused by an increase in joint spacing (8.36 m-33.04 m). On the other hand, when the joint spacing is constant, an increase in joint friction causes an increase in MRCS. When joint spacing = 1 m, if the joint friction increases from 10° to 40° , MRCS increases by 564.92% (from 1.27 m to 8.36 m), and when joint spacing = 5 m, this increase in the joint friction angle causes a 606.24% increase in MRCS (4.68 m-33.05 m).

Finally, Figure 27d shows the effect of joint inclination and joint spacing depth on MRCS. Based on this figure, it can be seen that when joint inclination = 25° , an increase in joint spacing from 1 m to 5 m causes a 371.68% increase in MRCS

(from 5.79 m to 27.30 m); while joint inclination = 70° , this increase in joint spacing causes a 154.27% increase in the MRCS (10.56 m-26.85 m). Moreover, as it is depicted in Figure 10b, while the joint spacing is constant, an increase in joint inclination increases MRCS. When joint spacing = 1 m, an increase in the joint inclination from 25° to 70° causes an 82.44% increase in the MRCS (from 5.79 m to 10.59 m); and when joint spacing = 5 m, this increase in joint inclination causes a 1.65% decrease in MRCS (from 27.30 m to 26.85 m).

5. Conclusions

The influence of each independent variable, i.e. joint set number, undercut depth, joint friction, joint spacing, and joint inclination on MRCS was investigated. The result shows that an increase in the joint set number from 1 to 3 decreases MRCS from 10.47 m to 7.35 m by 29.77%. In addition, increasing undercut depth from 50 m to 400 m causes a 50.94% decrease in MRCS (from 14.52 m to 7.12 m). However, with an increase in joint spacing from 1 m to 5 m, MRCS rises from 3.09 m to 14.75 by 376.73%. It is noticeable that an increase of joint friction from 10° to 40° leads to an increase of 638.70% in MRCS (from 2.58 m to 19.10 m). The variation of MRCS versus joint inclination (from 25 to 70 degrees) is non-linear, showing a minimum at 45 degrees.

RSM analysis shows that while undercut depth is constant, an increase in the joint spacing number has a negative effect on MRCS. Also while joint friction is constant, an increase in the undercut depth has a negative effect on MRCS. The result shows while the undercut depth is constant, an increase in joint friction increases MRCS; while the joint friction angle is constant, an increase in the joint spacing has a positive effect on MRCS. Based on the result, it can be seen that when joint inclination = 25° , an increase in joint spacing from 1 m to 5 m causes an 371.68% increase in MRCS; while joint inclination = 70° , this increase in joint spacing causes a 154.27% increase in MRCS (10.56 m-26.85 m).

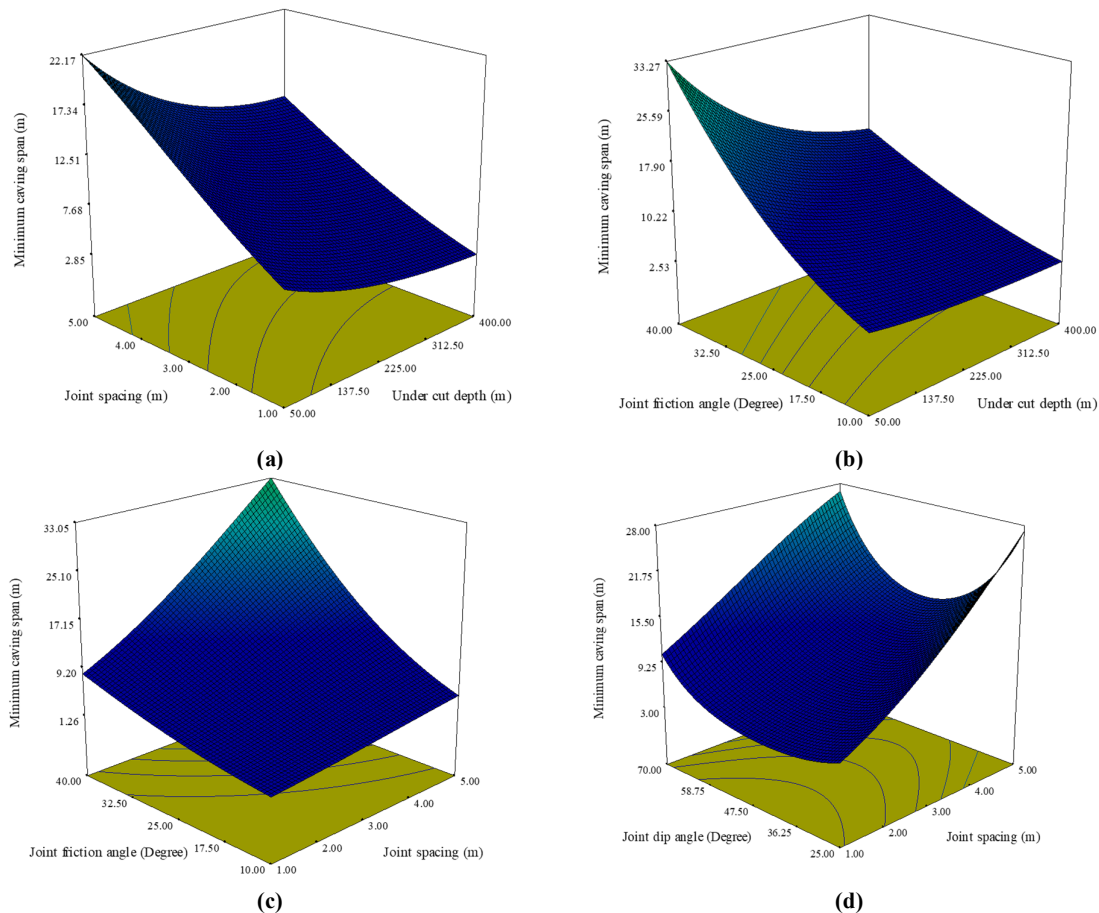


Figure 27. Mutual effects of rock mass parameters on MRCS a) effect of joint spacing and undercut depth b) effect of joint friction angle and undercut depth c) effect of joint friction angle and joint spacing d) effect of joint dip angle and joint spacing.

Conflict of Interest

The authors declare that they have no conflict of interest.

References

- [1]. Brady, B.H., and Brown, E.T. (2006). Rock mechanics: for underground mining. Springer science & business media.
- [2]. Mawdesley, C.A. (2002). Predicting rock mass cavability in block caving mines.
- [3]. Brannon, C.A., Carlson, G.K., and Casten, T.P. (2011). Block Caving & Cave Mining. SME Mining Engineering Handbook, 1437-1450.
- [4]. Rice, G. S. (1934). Ground movement from mining in Brier Hill mine, Norway, Michigan. Mining and Metallurgy. 15 (325): 12-14.
- [5]. Panek, L.A. (1984). Subsidence in undercut-cave operations, subsidence resulting from limited extraction of two neighboring-cave operations. Geomechanical applications in hard rock mining, 225-240.
- [6]. Beck, D., Sharrock, G., and Capes, G. (2011). A coupled DFE-Newtonian Cellular Automata scheme for simulation of cave initiation, propagation and induced seismicity. 45th US Rock Mechanics/Geomechanics Symposium. American Rock Mechanics Association.
- [7]. Carlson, G., and Golden, R. (2008). Initiation, Growth, Monitoring and Management of the 7210 Cave at Henderson Mine---A Case Study. In 5th International Conference and Exhibition on Mass Mining (Vol. 9, pp. 97-106).
- [8]. Ross, I., and Van As, A. (2005). Northparkes Mines-design, sudden failure, air-blast and hazard management at the E26 block cave. In 9th AusIMM Underground Operators Conference 2005 (Vol. 2005, No. 1, pp. 7-18). AUSTRALASIAN INST MINING & METALLURGY.
- [9]Somehnehsin, J., Oraee-Mirzamani, B., and Oraee, K. (2015). Analytical model determining the optimal block size in the block caving mining method. Indian Geotechnical Journal. 45 (2): 156-168.
- [10]. Raffee, R., Ataei, M., and KhalooKakaie, R. (2015). A new cavability index in block caving mines

- using fuzzy rock engineering system. *International Journal of Rock Mechanics and Mining Sciences*, 77, 68-76.
- [11]. Rafiee, R., Ataei, M., KhaloKakaie, R., Jalali, S. E., and Sereshki, F. (2016). A fuzzy rock engineering system to assess rock mass cavability in block caving mines. *Neural Computing and Applications*. 27 (7): 2083-2094.
- [12]. Mathews, K.E, Hoek, E., Wyllie, D.C, and Stewart, S. (1981). Prediction of stable excavation spans for mining at depths below 1000 m in hard rock.
- [13]. Tobie, R.L. and Julin, D. E. (1984). Block Caving: General Description in *Underground Mining Methods Handbook*, W. A. Hustrulid, ed., Soc. Mng. Enngr, New York, pp. 967-972.
- [14]. Laubscher, D. (2000). *Cave Mining Handbook*.
- [15]. Milne, D., Hadjigeorgiou, J., and Pakalnis, R. (1998). Rock mass characterization for underground hard rock mines. *Tunnelling and underground space technology*. 13 (4): 383-391.
- [16]. Palma, R., and Agarwal, R. (1973). A study of the cavability of primary ore at the El Teniente Mine. Technical Report from Colombia University, New York.
- [17]. Lorig, L. (2000). The Role of Numerical Modelling in Assessing Cavability. Itasca Consulting Group, Inc., Report to the International Caving Study. ICG00-099-3-16, October 22-25 (niepublikowane).
- [18]. Brown, E.T. (2002). Block caving geomechanics.
- [19]. Brown, E.T. (2003). Block Caving Geomechanics. The International Caving Study I. JKMRM Monograph Series in Mining and Mineral Processing 3. University of Queensland.
- [20]. Pierce, M., Cundall, P., Potyondy, D., and Ivars, D.M. (2007, May). A synthetic rock mass model for jointed rock. In 1st Canada-US Rock Mechanics Symposium. OnePetro.
- [21]. Ivars, D.M., Pierce, M.E., Darcel, C., Reyes-Montes, J., Potyondy, D.O., Young, R.P., and Cundall, P.A. (2011). The synthetic rock mass approach for jointed rock mass modelling. *International Journal of Rock Mechanics and Mining Sciences*. 48 (2): 219-244.
- [22]. Sainsbury, B. (2012). A model for cave propagation and subsidence assessment in jointed rock masses. University of South Wales.
- [23]. Woo, K.S., Eberhardt, E., Rabus, B., Stead, D., and Vyazmensky, A. (2012). Integration of field characterisation, mine production and InSAR monitoring data to constrain and calibrate 3-D numerical modelling of block caving-induced subsidence. *International Journal of Rock Mechanics and Mining Sciences*, 53, 166-178.
- [24]. Rafiee, R., Ataei, M., KhalooKakaie, R., Jalali, S.E., Sereshki, F., and Noroozi, M. (2018). Numerical modeling of influence parameters in cavability of rock mass in block caving mines. *International Journal of Rock Mechanics and Mining Sciences*, 105, 22-27.
- [25]. Xia, Z., Tan, Z., Pei, Q., and Wang, J. (2019). Ground pressure damage evolution mechanism of extraction level excavations induced by poor undercutting in block caving method. *Geotechnical and Geological Engineering*. 37 (5): 4461-4472.
- [26]. Xia, Z., Tan, Z., and Miao, Y. (2020). Damage evolution extraction structure during mining gently dipped orebody by block caving method. *Geotechnical and geological engineering*. 38 (4): 3891-3902.
- [27]. Wang, J., Wei, W., Zhang, J., Mishra, B., and Li, A. (2020). Numerical investigation on the caving mechanism with different standard deviations of top coal block size in LTCC. *International Journal of Mining Science and Technology*. 30 (5): 583-591.
- [28]. Mohammadi, S., Ataei, M., and Kakaie, R. (2018). Assessment of the importance of parameters affecting roof strata cavability in mechanized longwall mining. *Geotechnical and Geological Engineering*. 36 (4): 2667-2682.
- [29]. McNearney, R.L., and Abel Jr, J.F. (1993, April). Large-scale two-dimensional block caving model tests. In *International journal of rock mechanics and mining sciences & geomechanics abstracts* (Vol. 30, No. 2, pp. 93-109). Pergamon.
- [30]. Carmichael. P. and Hebblewhite. B. (2012). An investigation into semi-intact rock mass representation for physical modelling block caving mechanics' zone. Mining education Australian Research projects review.
- [31]. Cumming-Potvin, D., Wesseloo, J., Jacobsz, S. W., and Kearsley, E. (2016). Fracture banding in caving mines. *Journal of the Southern African Institute of Mining and Metallurgy*. 116 (8): 753-761.
- [32]. Obert, L., E. (1973). Design and Stability of Excavation, Sec. 7 in *SME Mining Engineering Handbook*, A. B. Cummins and I. A. Given, Ed., Soc. Mng. Enngr, New York, p. 49.
- [33]. Darling, P. (Ed.). (2011). *SME mining engineering handbook* (Vol. 1). SME.
- [34]. Jakubec, J. and E. (2007). Use of the Mining Rock Mass Rating (MRMR) Classification, *Proceedings of the International Workshop on Rock Mass Classification in Underground Mining*, pp. 73-78.
- [35]. Suorineni, F.T. (2010). The stability graph after three decades in use: experiences and the way forward. *International journal of mining, Reclamation and Environment*. 24 (4): 307-339.
- [36]. Vakili, A., and Hebblewhite, B.K. (2010). A new cavability assessment criterion for longwall top coal

caving. *International Journal of Rock Mechanics and Mining Sciences*. 47 (8): 1317-1329.

[37]. Brummer, R.K. (2005). The South African Institute of Mining and Metallurgy International Symposium on Stability of Rock Slopes in Open Pit Mining and Civil Engineering, pp. 411–420.

[38]. Gilbride, L.J., Free, K.S., and Kehrman, R. (2005, June). Modeling Block Cave Subsidence at the Molycorp, Inc., Questa Mine? A Case Study. In *Alaska Rocks 2005, The 40th US Symposium on Rock Mechanics (USRMS)*. OnePetro.

[39]. Vyazmensky, A., Elmo, D., and Stead, D. (2010). Role of rock mass fabric and faulting in the development of block caving induced surface subsidence. *Rock mechanics and rock engineering*. 43 (5): 533-556.

[40]. Montgomery, D.C. (2001). *Design and analysis of experiments*. John Wiley & Sons. Inc., New York, 1997, 200-1.

[41]. Kirmizakis, P., Tsamoutsoglou, C., Kayan, B., and Kalderis, D. (2014). Subcritical water treatment of landfill leachate: Application of response surface methodology. *Journal of environmental management*. 146: 9-15.

[42]. Sodeifian, G.H., Azizi, J., and Ghoreishi, S.M. (2014). Response surface optimization of *Smyrnum cordifolium* Boiss (SCB) oil extraction via supercritical carbon dioxide. *The Journal of Supercritical Fluids*. 95: 1-7.

[43]. Yuan, Z., Yang, J., Zhang, Y., and Zhang, X. (2015). The optimization of air-breathing micro direct methanol fuel cell using response surface method. *Energy*. 80: 340-349.

[44]. Asadizadeh, M., Moosavi, M., Hossaini, M.F., and Masoumi, H. (2018). Shear strength and cracking process of non-persistent jointed rocks: an extensive experimental investigation. *Rock Mechanics and Rock Engineering*. 51 (2): 415-428.

[45]. Heidarzadeh, S., Saeidi, A., and Rouleau, A. (2018). Assessing the effect of open stope geometry on rock mass brittle damage using a response surface methodology. *International Journal of Rock Mechanics and Mining Sciences*, 106, 60-73.

[46]. Rastbood, A., Gholipour, Y., and Majdi, A. (2017). Finite element-based response surface methodology to optimize segmental tunnel lining. *Engineering, Technology & Applied Science Research*. 7 (2): 1504-1514.

[47]. Asadizadeh, M., Moosavi, M., and Hossaini, M.F. (2018). Investigation of the mechanical behaviour of non-persistent jointed blocks under uniaxial compression. *Geomech. Eng.* 14 (1): 29-42.

[48]. Miller, D.M. (1984). Reducing transformation bias in curve fitting. *The American Statistician*. 38 (2): 124-126.

ارزیابی قابلیت تخریب توده‌سنگ در روش استخراج تخریب بلوکی با استفاده از شبیه‌سازی عددی و روش سطح پاسخ

بهنام علی پنهانی، عباس مجدی* و حسن بخشنده امنیه

بخش مهندسی معدن، دانشگاه تهران، تهران، ایران

ارسال ۲۰۲۲/۰۴/۲۵، پذیرش ۲۰۲۲/۰۶/۳۰

* نویسنده مسئول مکاتبات: amajdi@ut.ac.ir

چکیده:

هدف از این مقاله استفاده از روش سطح پاسخ (RSM) به منظور ارائه یک مدل آماری برای تخمین حداقل دهانه تخریب (MRCS) و برآورد تاثیرات مجزاء و متقابل پارامترهای توده‌سنگ بر روی قابلیت تخریب آن است. داده‌های مورد نیاز از نتایج مدل‌سازی عددی به دست آمده است. در این مقاله، شبیه‌سازی‌های عددی متنوعی (۴۸۰ مدل) با استفاده از نرم‌افزار UDEC به منظور بررسی کامل قابلیت تخریب توده‌سنگ انجام شده است. تأثیر هر پارامتر به صورت جداگانه و متقابل بر MRCS با استفاده از آنالیز ANOVA بررسی شده است. ANOVA نشان می‌دهد که تمام پارامترهای انتخاب شده (عمق، شیب درزه، تعداد دسته درزه‌ها، زاویه اصطکاک سطح درزه و فاصله‌داری درزه) به شدت بر MRCS تأثیر می‌گذارد. به عبارت دیگر، نتایج ANOVA مطابقت بالایی با نتایج تحلیل حساسیت مرسوم دارد. علاوه بر این، ترکیب فاصله‌داری درزه و شیب آن بیشترین تأثیر متقابل را بر MRCS دارد و ترکیبی از عمق زیر برش و فاصله‌داری درزه کمترین تأثیر را بر MRCS دارد.

کلمات کلیدی: تخریب بلوکی، مدل‌سازی عددی، خصوصیات درزه، نرم‌افزار UDEC، روش سطح پاسخ.
